Supplementary Information

De novo synthesis of mesoporous titanium(IV)-organic frameworks with MIL-100 topology

Javier Castells-Gil,[a] Natalia M. Padial,[a,b] Neyvis Almora-Barrios,[a] Ivan da Silva,[c] Diego Mateo,[d] Josep Albero,[d] Hermenegildo García[d] and Carlos Martí-Gastaldo[a]*

[a]Universidad de Valencia (ICMol), Catedrático José Beltrán-2, 46980, Paterna (Spain).
[b]Department of Chemistry, The Scripps Research Institute, 10550 North Torrey Pines Road, La Jolla, California 92037, (United States).
[c]ISIS Facility, Rutherford Appleton Laboratory, Chilton, Didcot, Oxfordshire, OX11 0QX (United Kingdom).
[d]Instituto Universitario de Tecnología Química CSIC-UPV, Universitat Politècnica de València, Av. De los Naranjos s/n, 46022, Valencia (Spain).

S1. Materials and reagents.

$Ti(O^iPr)_4$ (97%), Cp_2TiCl_2 (97%), $CpTiCl_3$(97%), 4-tert-butyl-benzoic acid (98%), benzoic acid (98%), methanol (anhydrous, 99.9%), isopropanol (99.9%), tetrahydrofurane, (anhydrous, 99.9%) *N,N*-dimethylformamide (anhydrous, 99.8%), and acetic acid (99.97%) were purchased from Sigma-Aldrich. Acetonitrile (anhydrous, 99.9%), *N,N*-diethylformamide and 1,3,5-benzene-trisbenzoic acid (98%) were purchased from Acros Organics and TCI Europe, respectively. All reagents and solvents were used as received without further purification.

S2. Synthesis of materials and experimental details.

Synthesis of $[Ti_6O_6(O^iPr)_6(4\text{-tbbz})_6]$ (4-tbbz = 4-*tert*-butylbenzoic acid; Ti_6): The synthesis of the Ti_6 cluster was carried out according to the previously reported procedure.[1]

Synthesis Optimization of MIL-100(Ti): We used a high-throughput ChemSpeed platform for robotic dispensing of solids and liquids. The following reaction parameters were systematically investigated:

- **Temperature**: Optimization of the reaction conditions were carried out by adding 7.2 mg of Ti_6 (24 µmol of Ti), 25.0 mg of H_3btc (120 µmol) to 3 mL of a mixture of ACN:THF (3:1, v/v %) in a capped glass vial. Subsequently, different amounts of acetic acid, i.e. 0, 250, 500 or 750 µL (0, 4.32, 8.64 and 12.96 mmol, respectively) were added and the mixture was sonicated to produce a homogeneous suspension. The vials were placed in the oven at different temperatures (80, 100, 120, 140 or 160 °C) for 48 hours. After cooling down to room temperature, the solids were separated by centrifugation and rinsed with fresh DMF (3x15 mL), methanol (2x15 mL) and washed by soxhlet extraction with hot methanol or ethanol for several hours. The solids were then allowed to dry under vacuum at room temperature.
- **Modulator:** Optimization of the reaction conditions were carried out by adding 7.2 mg of Ti_6 (24 µmol of Ti), 25.0 mg of H_3btc (120 µmol) to 3 mL of a mixture of ACN:THF (3:1, v/v %) in a capped glass vial. Subsequently, different amounts of acetic acid, i.e. 0, 250, 500 or 750 µL (0, 4.32, 8.64 and 12.96 mmol, respectively) were added and the mixture was sonicated to produce a homogeneous suspension. The vial was placed in the oven at 160 °C for 48 hours. After cooling down to room temperature, the solids were separated by centrifugation and rinsed with fresh DMF (3x15 mL), methanol (2x15 mL) and washed by soxhlet extraction with hot methanol or ethanol for several hours. The solids were then allowed to dry under vacuum at room temperature.
- **Ti:btc ratio:** Optimization of the reaction conditions were carried out by adding 7.2 mg of Ti_6 (24 µmol of Ti), and 5.0 (24 µmol, Ti:btc 1:1), 10.0 (48 µmol, Ti:btc 1:2), 15.0 (72 µmol, Ti:btc 1:3), 20.0 (96 µmol, Ti:btc 1:4) or 25.0 mg (120 µmol, Ti:btc 1:5) of H_3btc and 250 µL (4.32 mmol, 180 eq.) of acetic acid to 3 mL of a mixture of ACN:THF (3:1, v/v %) in a capped glass vial. Subsequently, the mixture was sonicated to produce a homogeneous suspension. The vial was placed in the oven at 160 °C for 48 hours. After cooling down to room temperature, the solids were separated by centrifugation and rinsed with fresh DMF (3x15 mL), methanol (2x15 mL) and washed by soxhlet extraction with hot methanol or ethanol for several hours. The solids were then allowed to dry under vacuum at room temperature.

Synthesis of MIL-100(Ti): A typical synthesis of MIL-100(Ti) was carried out by adding 7.2 mg of Ti_6 (24 µmol of Ti), 25.0 mg of H_3btc (120 µmol) to 3 mL of a mixture of ACN:THF (3:1, v/v %) and 250 µL (4.32 mmol, 180 eq.) of acetic acid in a capped glass vial. Subsequently, the mixture was sonicated to produce a homogeneous suspension. The vial was placed in the oven at 160 °C for 48 hours. After cooling down to room temperature, the solids were separated by centrifugation and rinsed with fresh DMF (3x15 mL), methanol (2x15 mL) and washed by soxhlet extraction with hot methanol or ethanol for several hours. The solids were then allowed to dry under vacuum at room temperature.

Synthesis of MIL-100(Ti) from simple metal precursors (Cp_2TiCl_2, $CpTiCl_3$, $Ti(O^iPr)_4$): The synthesis of MIL-100(Ti) from simple Ti(IV) precursors was carried out by adding 24 µmol of Ti, 25.0 mg of H_3btc (120 µmol) to 3 mL of a mixture of ACN:THF (3:1, v/v %) in a glass vial. Subsequently, 500 µL of acetic acid were added and the mixture was sonicated to get a homogeneous suspension. The vial was placed in the oven at 160 °C for 12 hours. After cooling down to room temperature, the solids were separated by centrifugation and rinsed with fresh DMF (3x15 mL), methanol (2x15 mL) and washed by soxhlet extraction with hot methanol or ethanol for several hours. The solids were then allowed to dry under vacuum at room temperature.

Synthesis of MIL-125: MIL-125 was synthesized by dissolving in 500 mg (3.0 mmol) of terephthalic acid and 183 µL (0.6 mmol) of $Ti(O^iPr)_4$ in 20 mL of a DMF:MeOH (9:1 v/v %) mixture in a 25 mL Schott bottle. The solution was heated at 150 °C for 24 hours. The white solid formed was recovered by centrifugation and washed with fresh DMF (3x50 mL) and isopropanol (3x50 mL) and dried under vacuum at room temperature.

Synthesis of MIL-100(Fe): MIL-100(Fe) was synthesized according to a reported procedure.[2]

Systematic optimization of the reaction conditions.

The effect of the reaction temperature and concentration of modulator (acetic acid) on the formation of MIL-100(Ti) was evaluated by powder X-Ray diffraction (PXRD). PXRD of the solids were measured in a PANalytical Empyrean X-Ray diffractometer in transmission mode measurement by using a High-throughput platform. XRD patterns were collected in the angular range 3° < 2θ < 45 ° with a step size of 0.013°.

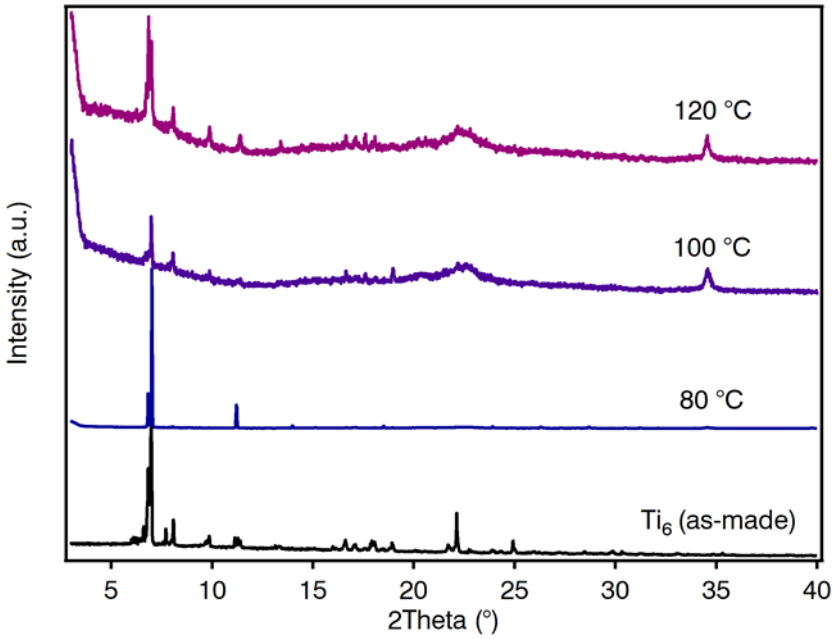

Figure S1. Comparison of PXRD of Ti_6 with those of the product obtained from the synthesis of MIL-100(Ti) at different reaction temperatures for V_{AcOH} = 0 µL.

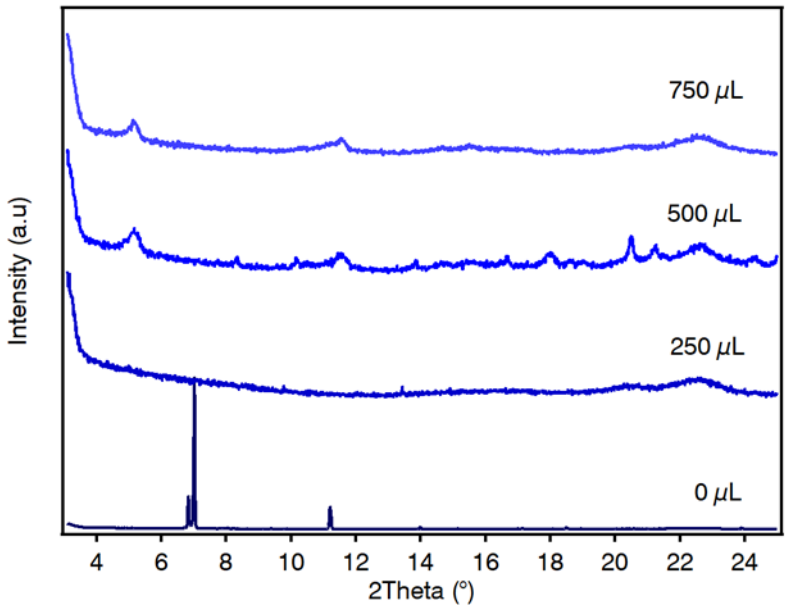

Figure S2. PXRD of MIL-100(Ti) synthesized at 80 °C with different amounts of acetic acid.

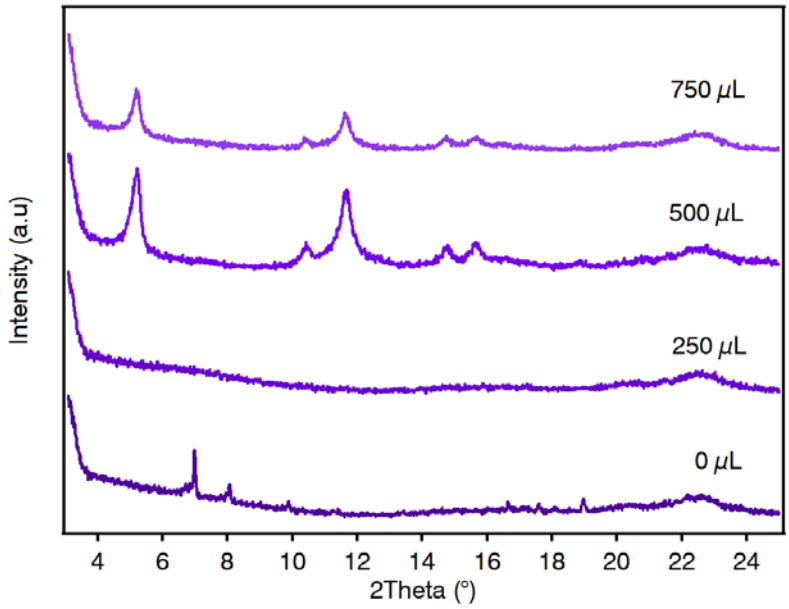

Figure S3. PXRD of MIL-100(Ti) synthesized at 100 °C with different amounts of acetic acid.

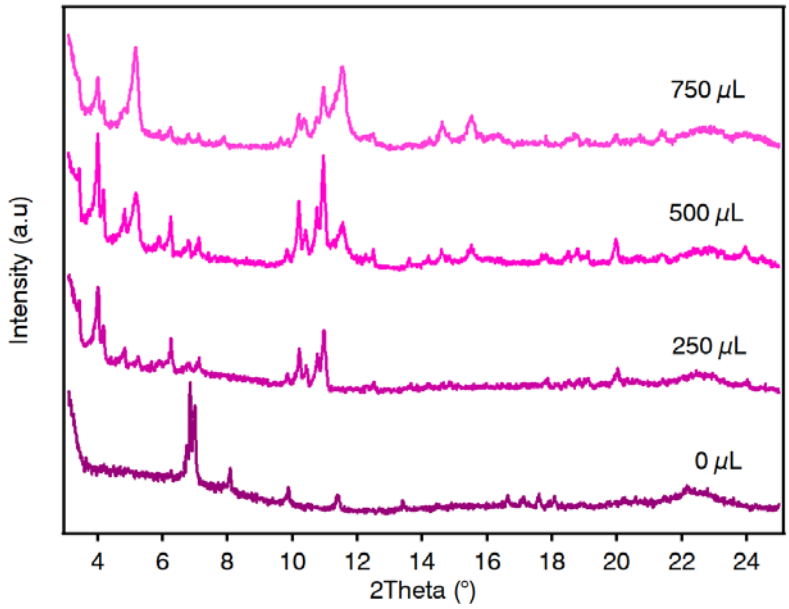

Figure S4. PXRD of MIL-100(Ti) synthesized at 120 °C with different amounts of acetic acid.

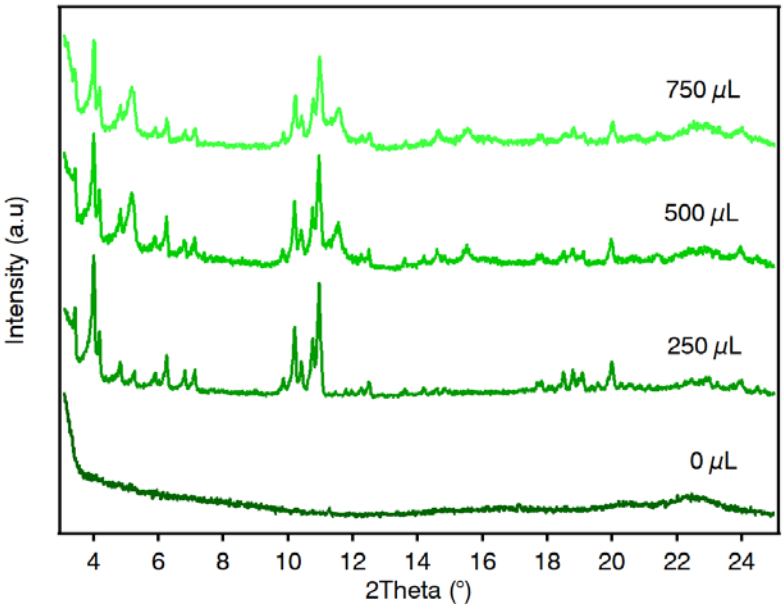

Figure S5. PXRD of MIL-100(Ti) synthesized at 140 °C with different amounts of acetic acid.

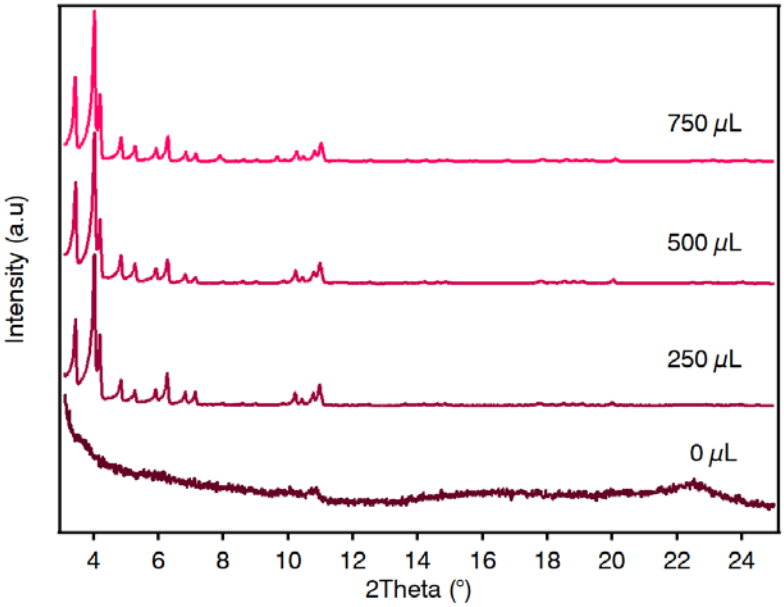

Figure S6. PXRD of MIL-100(Ti) synthesized at 160 °C with different amounts of acetic acid.

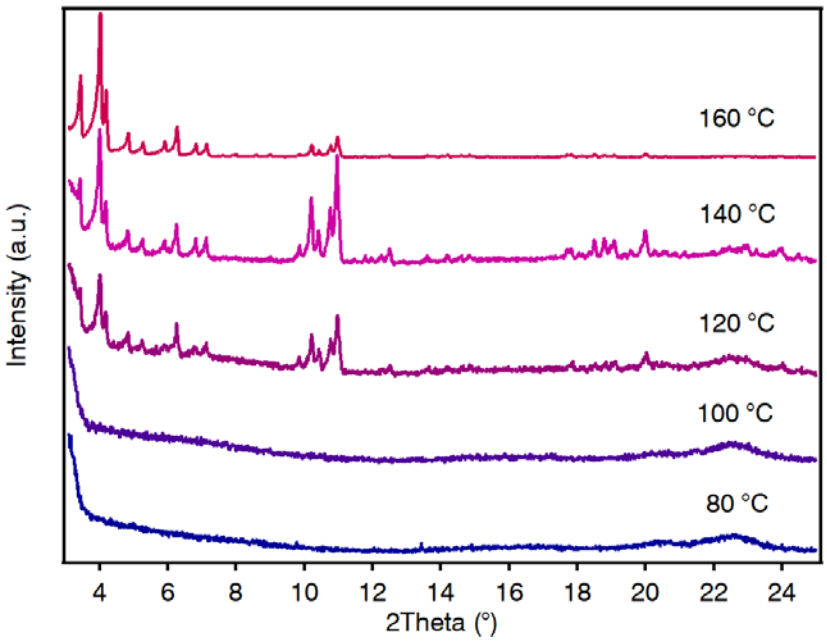

Figure S7. PXRD of MIL-100(Ti) synthesized at different reaction temperatures (V_{AcOH} = 250 µL).

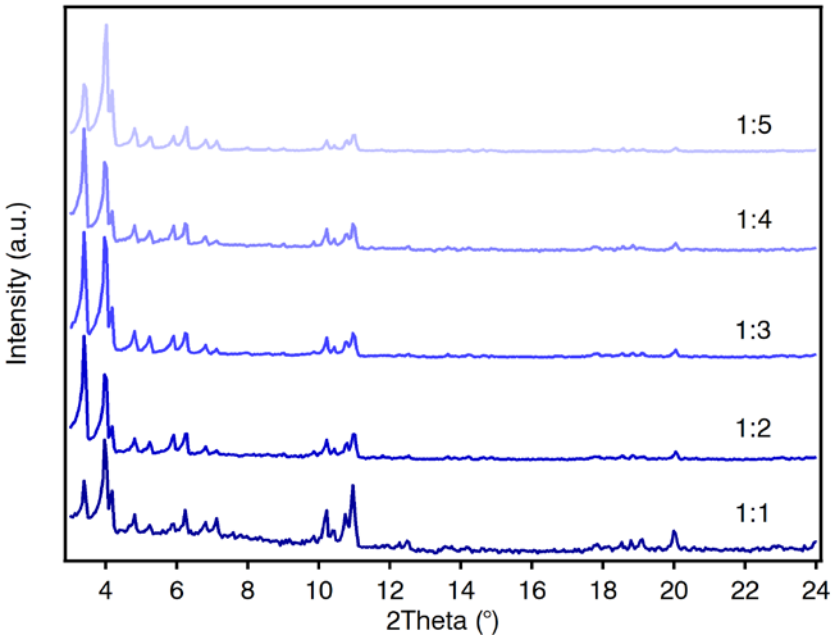

Figure S8. PXRD of MIL-100(Ti) synthesized at 160 °C with different Ti:btc ratios (V_{AcOH} = 250 µL).

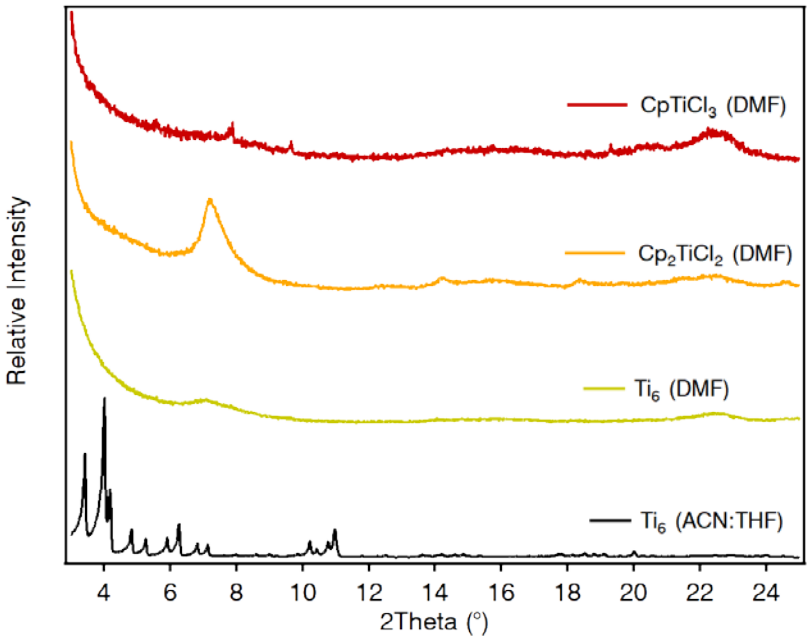

Figure S9. PXRD of the products obtained from the synthesis of MIL-100(Ti) in DMF with different Ti(IV) precursors (V_{AcOH} = 250 µL).

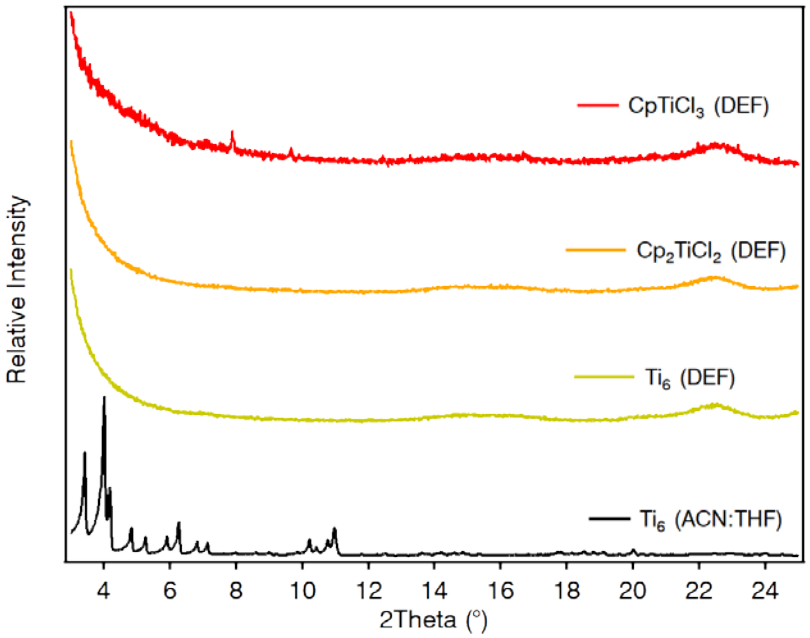

Figure S10. PXRD of the products obtained from the synthesis of MIL-100(Ti) in DEF with different Ti(IV) precursors (VAcOH = 250 µL).

S3. Chemical Characterization

Scanning Electron Microscopy (SEM-EDX)

Particle morphologies and dimensions were studied with a Hitachi S-4800 scanning electron microscope at an accelerating voltage of 20 kV, over metalized samples with a mixture of gold and palladium during 90 seconds.

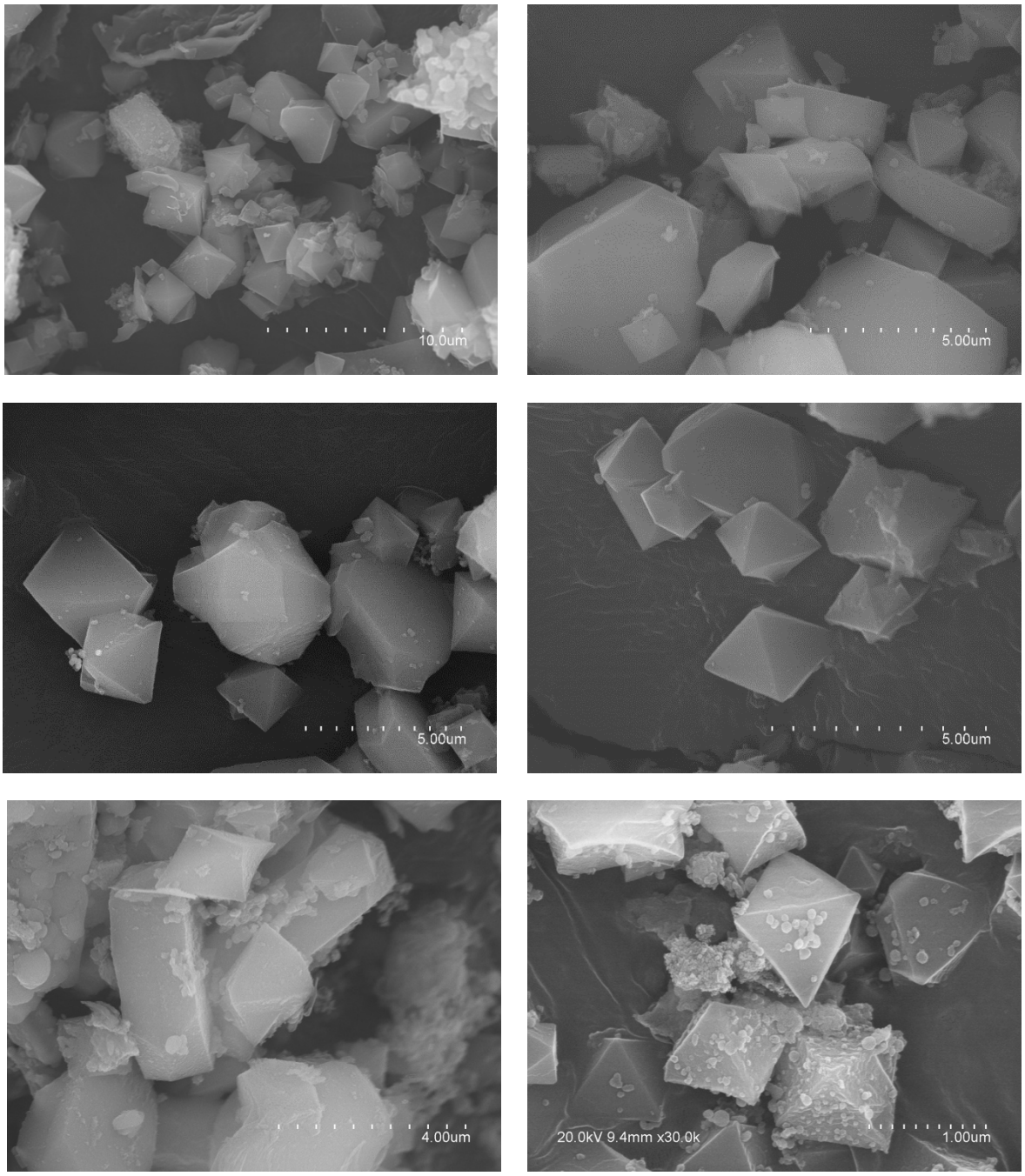

Figure S11. Scanning Electron Microscopy (SEM) images of octahedral crystals of MIL-100(Ti) synthesized from the metal cluster Ti_6. Higher magnification confirms the formation of a small fraction of an amorphous phase of the solid.

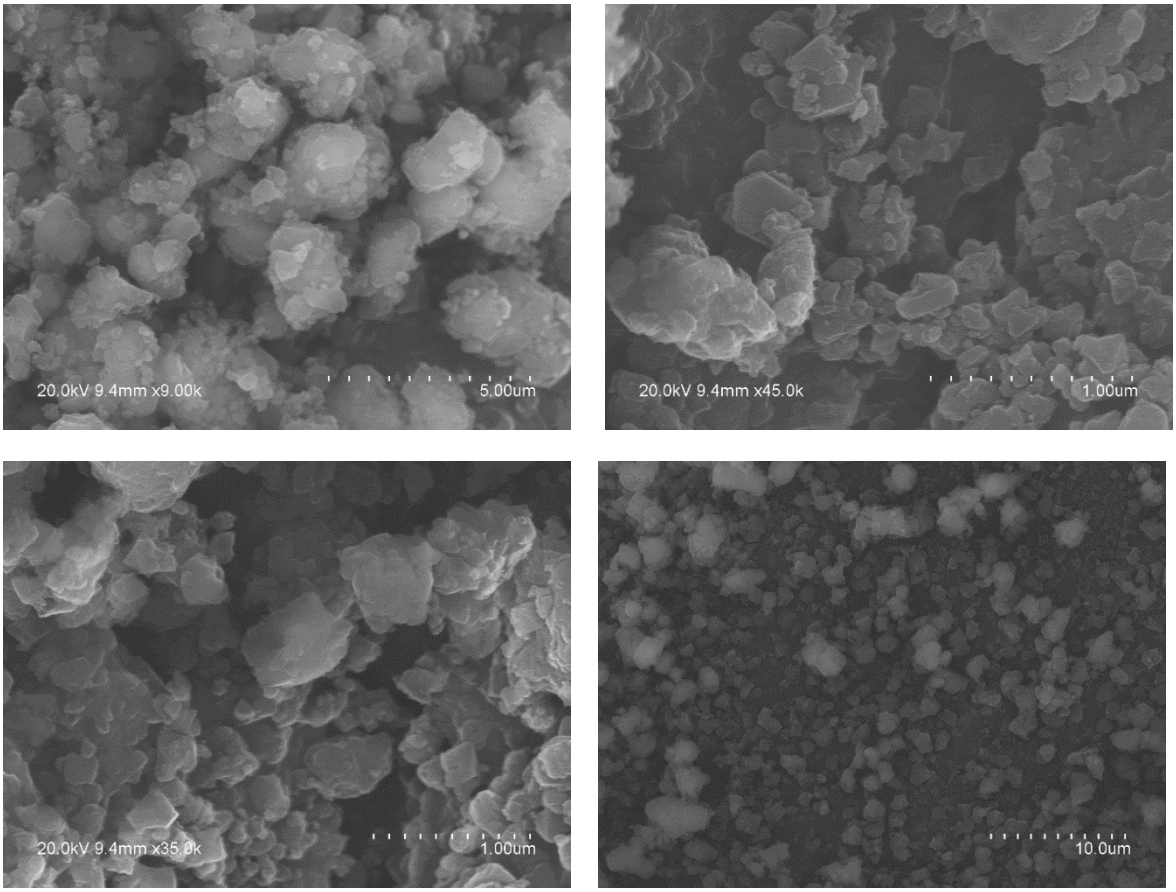

Figure S12. Scanning Electron Microscopy (SEM) images of MIL-100(Ti)-Cp_2TiCl_2.

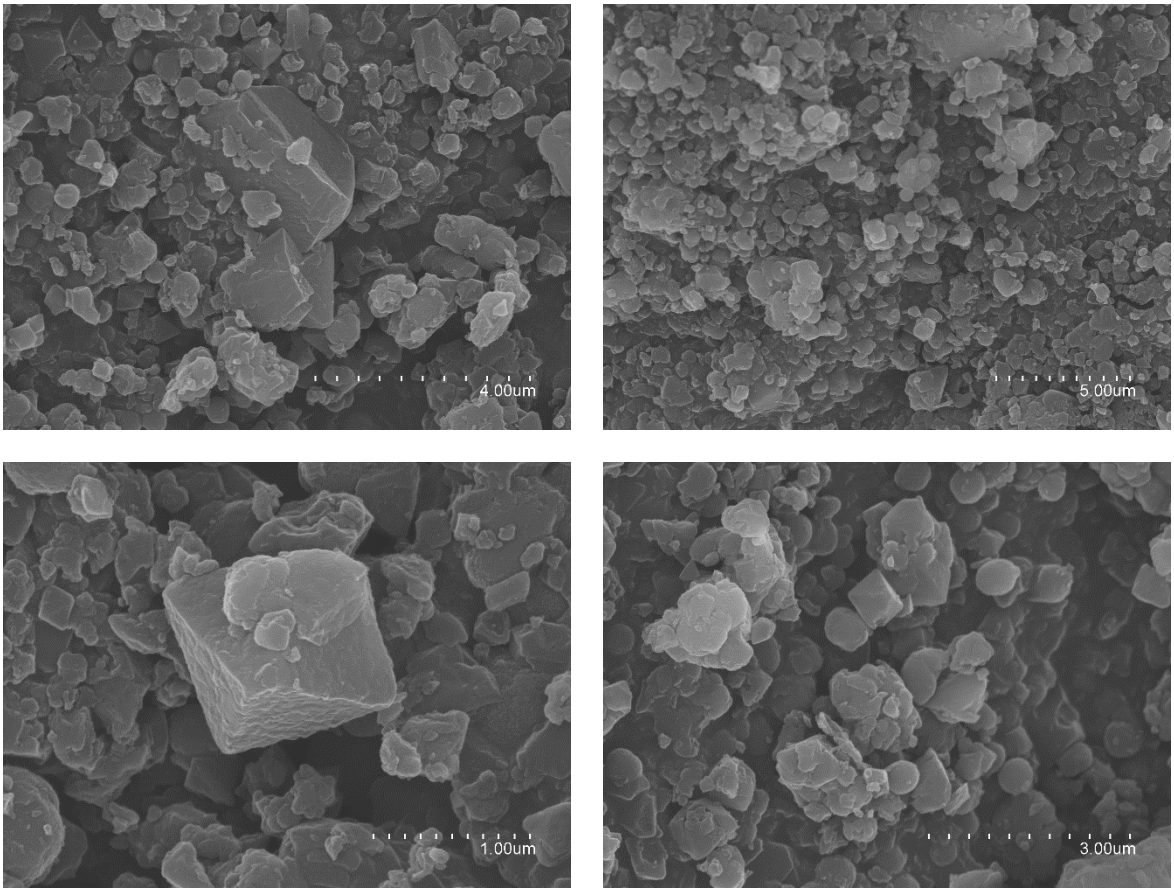

Figure S13. Scanning Electron Microscopy (SEM) images of MIL-100(Ti)-$CpTiCl_3$.

Rietveld refinement and crystallographic data of MIL-100(Ti).

The structural model of MIL-100(Fe) was used as starting point for a Rietveld refinement, which was carried out with Topas Academic 5 program (http://www.topas-academic.net/). The six crystallographically independent organic linkers were modelled using semi-rigid bodies, where selected bond distances, bond angles and torsion angles could be refined. In the case of non-activated MIL-100(Ti), ethanol molecules were described as rigid bodies, which could freely translate and rotate inside the pores. Background was fitted with a 17-coefficients Chebyshev polynomial and peak shapes were modelled with a Thompson-Cox-Hasting pseudo-Voigt profile function. Crystallographic parameters from the final Rietveld refinement are summarized in Table S1.

Table S1. Crystallographic data and Rietveld refinement of MIL-100(Ti)

Identification code	MIL-100(Ti) activated
CCDC Number	1871195
Empirical formula	$C_{306}H_{102}O_{272}Ti_{51}$, $40.92(C_2H_6O)$
Formula weight	12456.26
Cryst. Syst.	Cubic
Space group	Fd-3m
a, Å	73.5168(16)
V, Å3	397340(30)
Z	16
Temperature, K	298
Wavelength, Å	1.540596
2Θ range, °	2.5-70
Number of reflections	4081
Number of structural/total variables	118/140
Rp, %	3.86
Rwp, %	5.24
Rexp, %	1.93
GoF	2.72

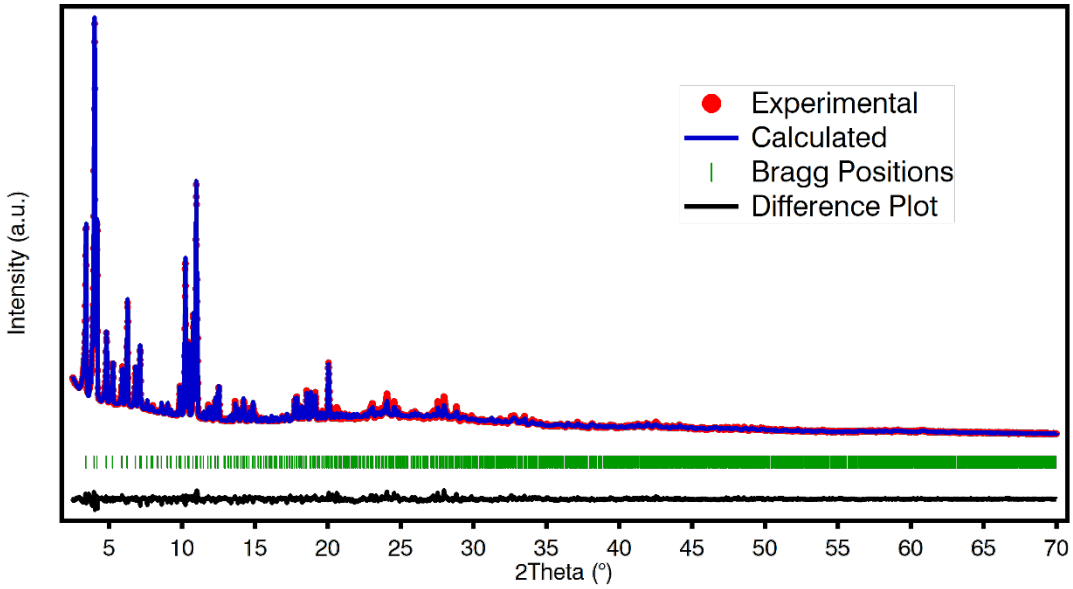

Figure S14. Experimental (red dots), calculated (blue line), difference plot [(*I*obs−*I*calc)] (black line, bottom panel) and Bragg positions (green ticks) for the Rietveld refinement of experimental diffraction data of non-activated MIL-100(Ti) collected at room temperature.

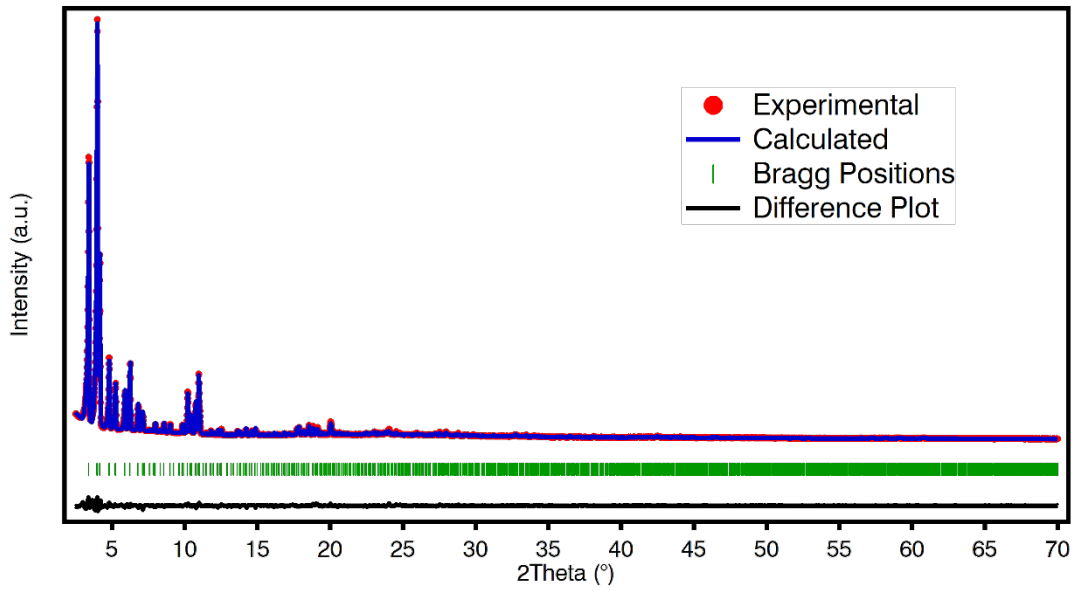

Figure S15. Experimental (red dots), calculated (blue line), difference plot [(*I*obs−*I*calc)] (black line, bottom panel) and Bragg positions (green ticks, bottom panel) for the Rietveld refinement of experimental diffraction data of activated MIL-100(Ti) collected at room temperature.

Powder X-Ray Diffraction (PXRD): LeBail refinements

Powder XRD patterns were collected for polycrystalline samples using a 0.5 mm glass capillary mounted and aligned in a PANalytical Empyrean diffractometer (Bragg-Brentano geometry) using copper radiation (Cu Kα = 1.5418 Å) with an PIXcel detector, operating at 40 mA and 45 kV. Profiles were collected by using a Soller Slit of 0.02° and a divergence slit of ¼ at room temperature in the angular range 2° < 2θ < 50° with a step size of 0.013°. LeBail refinements were carried out with the FULLPROF software package.

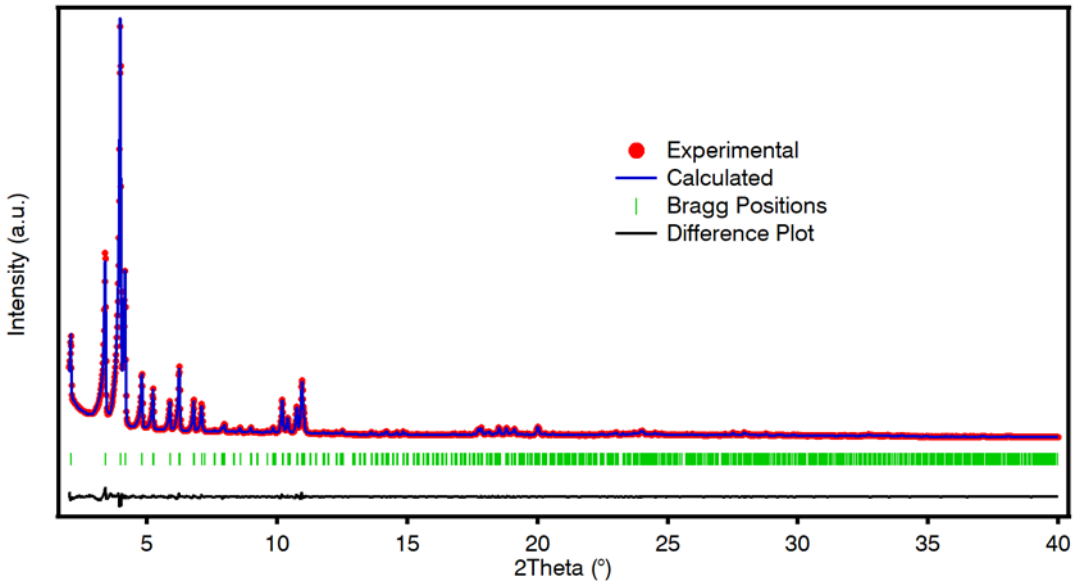

Figure S16. Experimental (red dots), calculated (blue line), difference plot [(*I*obs−*I*calc)] (black line, bottom panel) and Bragg positions (green ticks, bottom panel) for the LeBail refinement of experimental diffraction data of MIL-100(Ti) collected at room temperature.

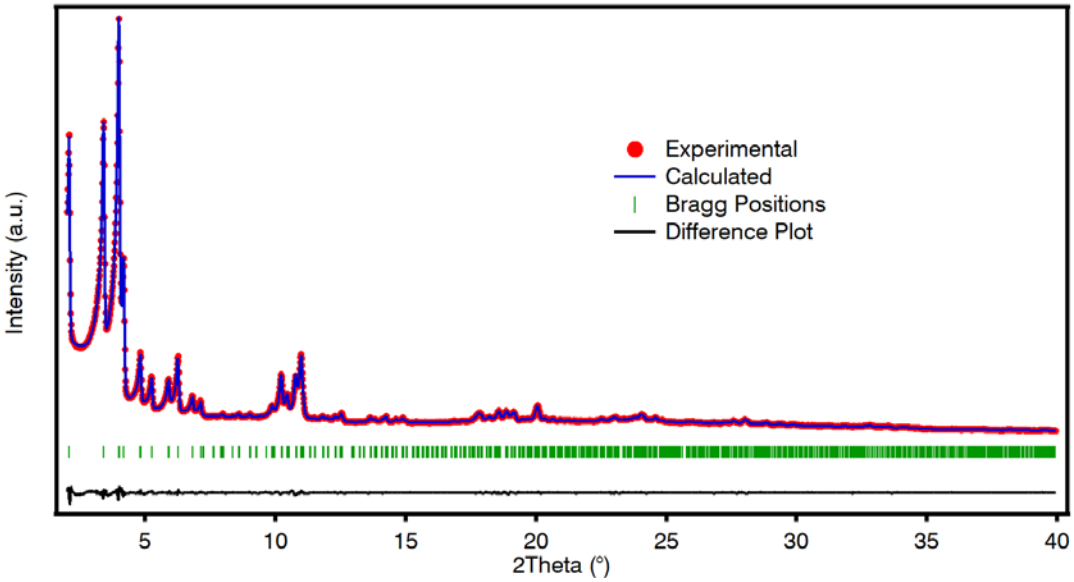

Figure S17. Experimental (red dots), calculated (blue line), difference plot [(*I*obs−*I*calc)] (black line, bottom panel) and Bragg positions (green ticks, bottom panel) for the LeBail refinement of experimental diffraction data of MIL-100(Ti)-Cp_2TiCl_2 collected at room temperature.

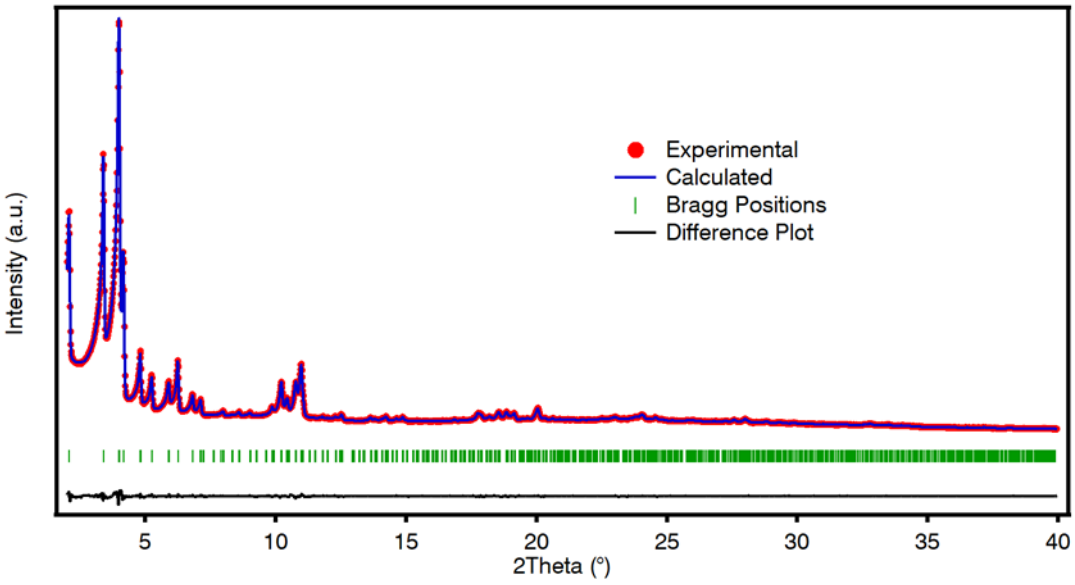

Figure S18. Experimental (red dots), calculated (blue line), difference plot [(*I*obs−*I*calc)] (black line, bottom panel) and Bragg positions (green ticks, bottom panel) for the LeBail refinement of experimental diffraction data of MIL-100(Ti)- $CpTiCl_3$ collected at room temperature.

Table S2. Summary of the parameters obtained from LeBail refinement.

Ti(IV) Precursor	a=b=c [Å]	V [Å^3]	R_e [%]	R_p [%]	R_{wp} [%]	gof
Ti_6	73.5314	397574	2.44	2.78	3.56	1.4
Cp_2TiCl_2	73.3367	394425	1.09	1.18	1.50	1.4
$CpTiCl_3$	73.3816	395149	1.14	1.43	1.11	1.3

Fourier Transformed Infrared Spectroscopy (FT-IR)

FT-IR spectra of MIL-100(Ti) solids were collected in the range 4000-650 cm^{-1} with an Agilent Cary 630 FTIR Spectrometer equipped with an ATR module.

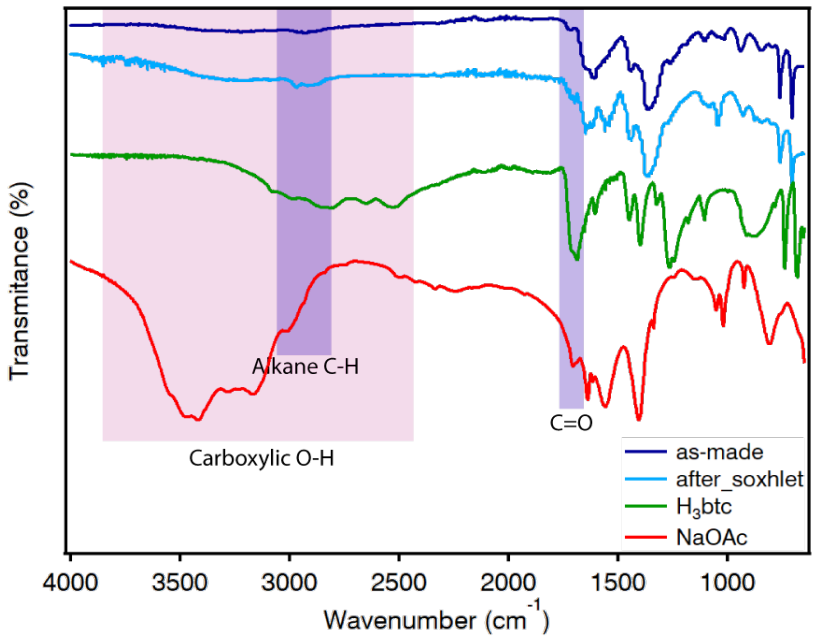

Figure S19. FT-IR spectra of MIL-100(Ti) before (blue) and after (cyan) washing by soxhlet with methanol compared to the spectra of sodium acetate (NaOAc, red) and trimesic acid (H_3btc, green).

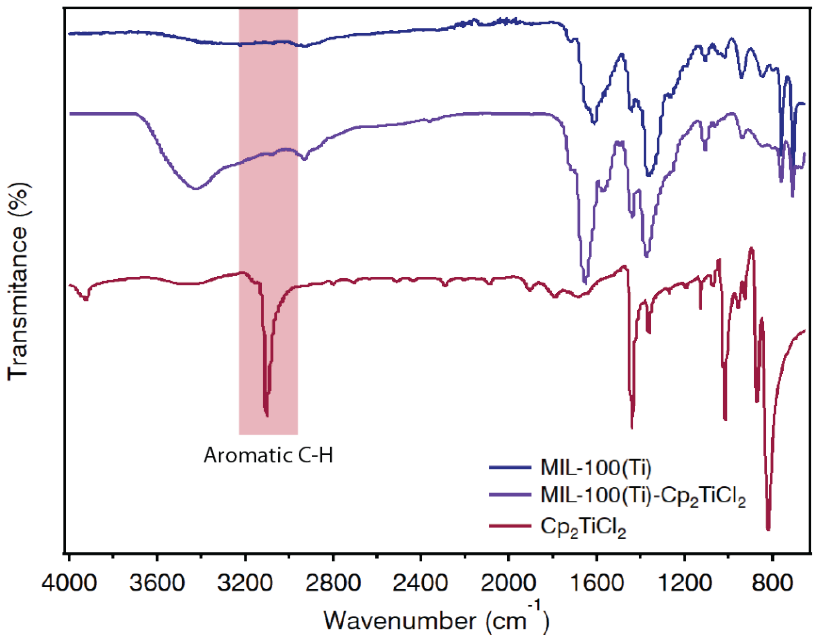

Figure S20. FT-IR of bare Cp_2TiCl_2 (red) compared to that of MIL-100(Ti) (blue) and MIL-100(Ti)-Cp_2TiCl_2 (purple).

Thermogravimetric Analysis (TG-SDTA)

TGA-SDTA curves were recorded at a ramp rate of 5 °C/min on a Mettler Toledo TGA/SDTA 851e/SF/1100 apparatus between 25 and 800 °C under synthetic air.

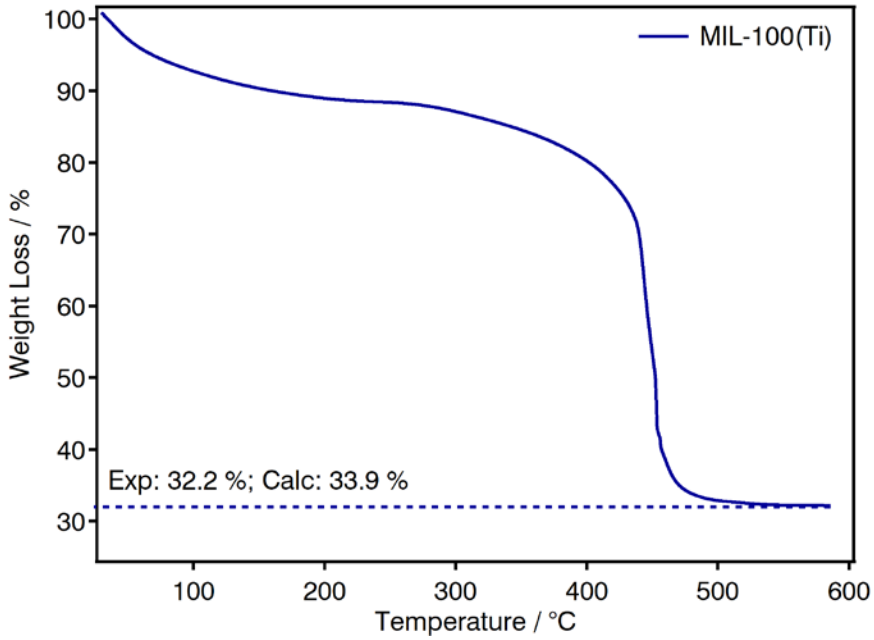

Figure S21. Thermogravimetric analysis (TGA) of MIL-100(Ti)

As it can be discerned from Figure S19 MIL-100(Ti) shows a weight loss before its decomposition at around 450 °C which occurs between 25 and 200 °C and is due to the loss of solvent molecules occluded in the pores after MeOH exchange. The resulting residue upon decomposition of the framework was found to be 32.2% (Calc (% TiO_2): 33.9%).

Analysis of N_2 adsorption/desorption isotherms at 77 K

Gas adsorption measurements were performed ex situ on MIL-100(Ti) solids washed by soxhlet in MeOH. Surface area, pore size and volume values were calculated from nitrogen adsorption-desorption isotherms (77 K) recorded on a Micromeritics 3Flex apparatus. Samples were degassed overnight at 150 °C and 10^{-6} Torr overnight prior to analysis. Brunauer-Emmett-Teller (BET) Surface area analysis were performed as recommended for microporous and mesoporous materials.[3]

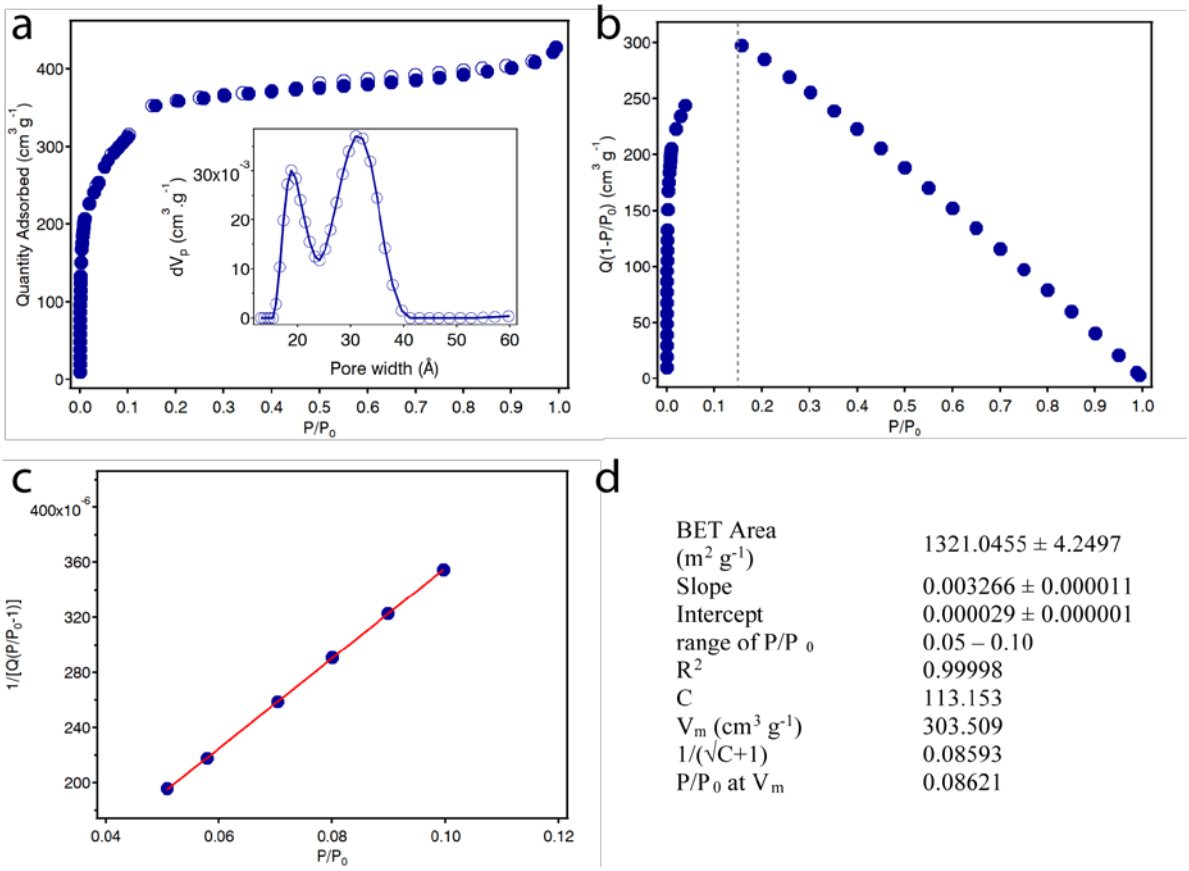

Figure S22. Analysis of the N_2 adsorption/desorption isotherm of MIL-100(Ti) at 77 K. a) N_2 adsorption isotherm (inset: Pore Size Distribution calculated by NLDFT), b) Rouquerol BET, c) Multi-Point BET analysis and d) main parameters calculated from the multi-point BET analysis of the as-madeMIL-100(Ti). The dashed line on (b) represents the limit of the applicability of the BET theory.

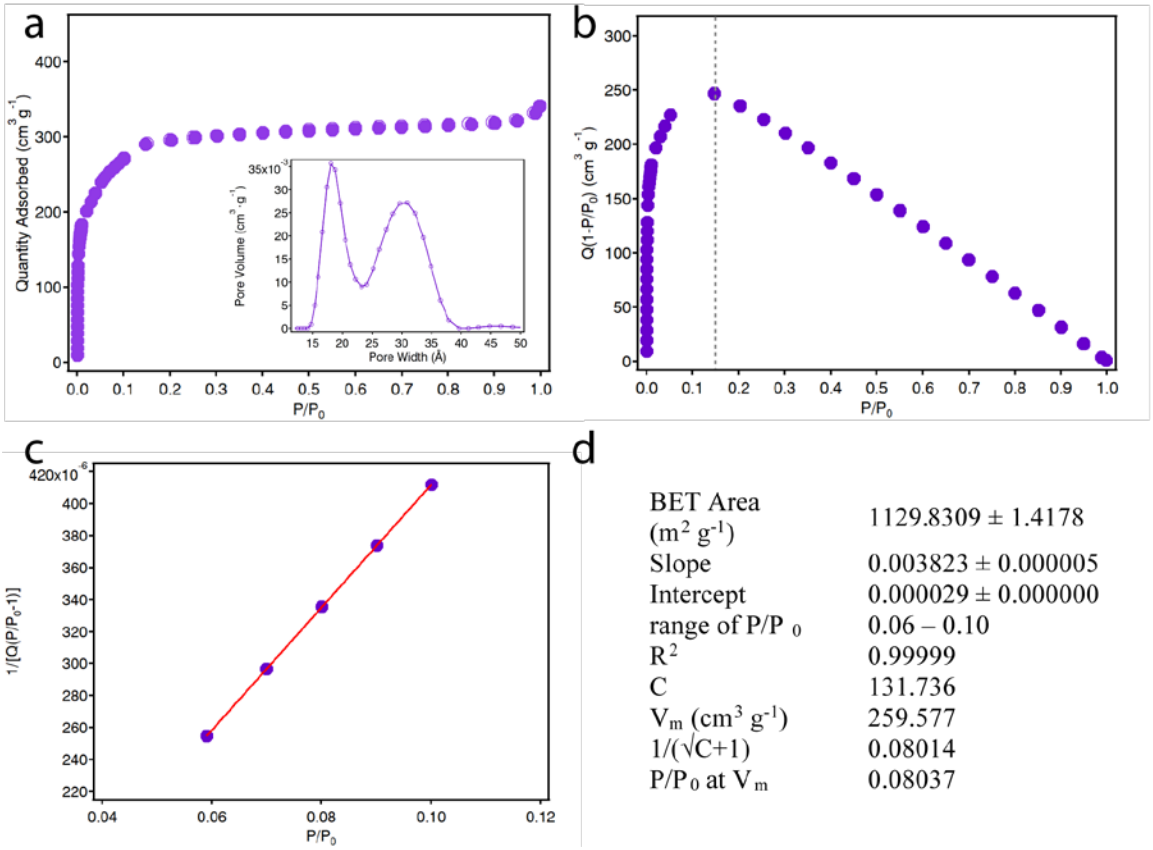

Figure S23. Analysis of the N_2 adsorption/desorption isotherm of MIL-100(Ti)- Cp_2TiCl_2 at 77 K. a) N_2 adsorption isotherm (inset: Pore Size Distribution calculated by NLDFT), b) Rouquerol BET, c) Multi-Point BET analysis and d) main parameters calculated from the multi-point BET analysis of the as-made MIL-100(Ti)-Cp_2TiCl_2. The dashed line on (b) represents the limit of the applicability of the BET theory.

Table S3. Main parameters obtained from N_2 adsorption isotherms of MIL-100(Ti) solids at 77 K.

Ti(IV) precursor	SA_{BET}[a] [$m^2 \cdot g^{-1}$]	V_t[b] [$cm^3 \cdot g^{-1}$]	PSD_{NLDFT}[c] [nm]	
Ti_6	1321	0.66	1.9	3.2
Cp_2TiCl_2	1130	0.51	1.8	3.1

[a]Specific surface area (SA) was calculated by multi-point Brunauer-Emmett-Teller (BET) method. [b]Total pore volume at P/P_0=0.96. [c]Pore size distribution was analysed by using the solid density functional theory (NLDFT) for the adsorption branch assuming a cylindrical pore model.

Analysis of CO_2 adsorption/desorption isotherms

Gas adsorption measurements were recorded on a Micromeritics 3Flex apparatus at relative pressures up to 1 atm and performed ex situ on MIL-100(Ti) solids washed by soxhlet in EtOH. Samples were degassed overnight at 150 °C and 10^{-6} Torr prior to analysis. A Micromeritics' ISO Controller was used to keep the temperature constant for the CO_2 adsoption measurements at 273, 283 and 293 K. The isosteric heats of adsorption were determined by means of the Clausius-Clapeyron equation as implemented in the MicroActive Analysis Software using the CO_2 isotherms recorded at 273, 283 and 293 K.

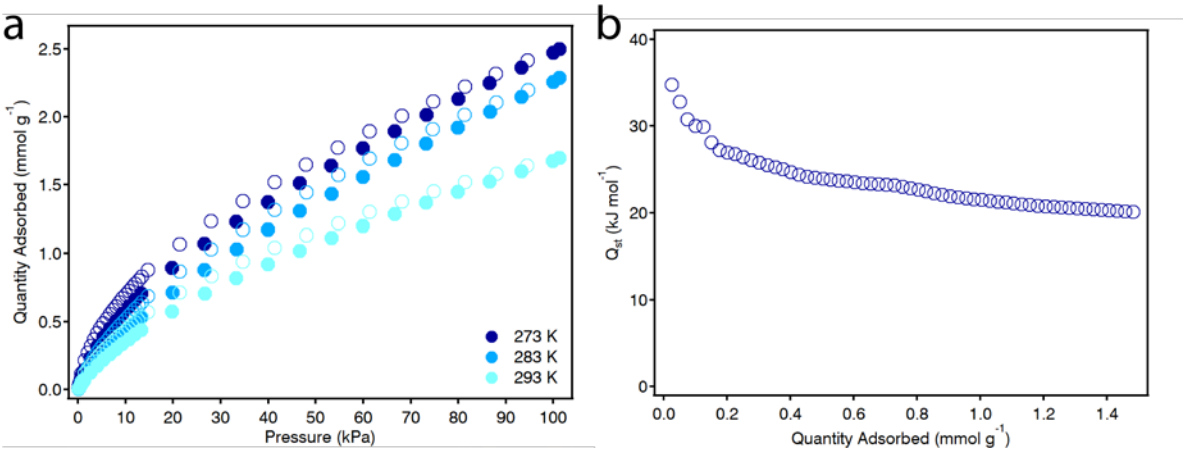

Figure S24. (a) CO_2 adsorption/desorption isotherms of MIL-100(Ti) recorded at different temperatures. (b) Isosteric heat of adsorption (Q_{st}) of MIL-100(Ti) calculated from the corresponding isotherms.

Analysis of H_2O adsorption/desorption isotherms

Gas adsorption measurements were recorded on a Micromeritics 3Flex apparatus at relative pressures up to 1 atm and performed ex situ on MIL-100(Ti) solids washed by soxhlet with EtOH or MeOH. Samples were degassed overnight at 150 °C and 10^{-6} Torr prior to analysis. A Micromeritics' ISO Controller was used to keep the temperature constant for the H_2O adsoption measurements at 298 K.

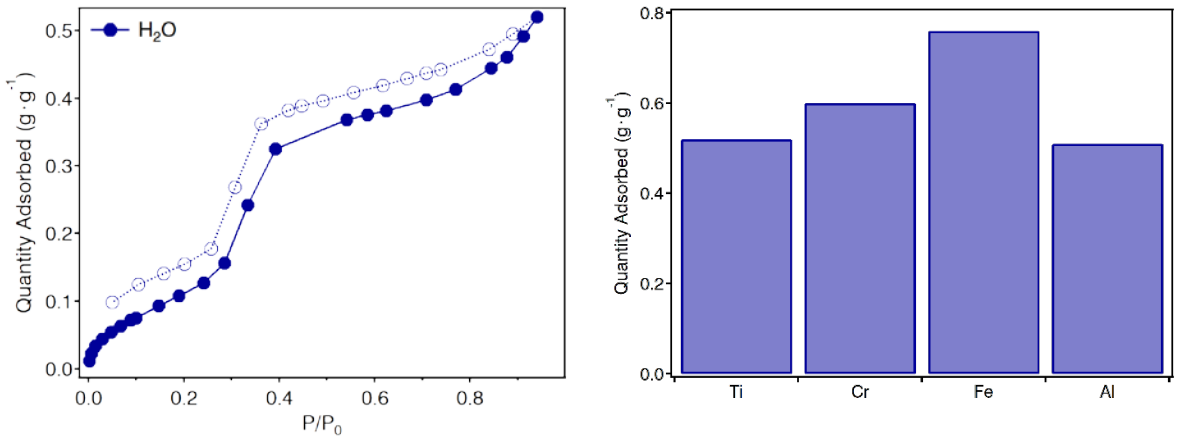

Figure S25 – Water adsorption isotherm of MIL-100(Ti) (left) performed at 298 K and comparison of the maximum water adsorption capacity at $P/P_0 = 0.9$ for different MIL-100(M) materials (M = Ti(IV), Cr(III), Fe(III) and Al(III)).

Table S4 – Maximum water adsorption capacity (q_{max}) at $P/P_0 = 0.9$ and range of relative pressure at which the steep water uptake takes place for different MIL-100 materials.

MIL-100(M)	q_{max} ($g \cdot g^{-1}$)	Steep Uptake	Reference
Ti	0.52	$0.25 < P/P_0 < 0.40$	[This work]
Cr	0.60	$0.30 < P/P_0 < 0.60$	[4]
Fe	0.76	$0.30 < P/P_0 < 0.45$	[5]
Al	0.51	$0.25 < P/P_0 < 0.45$	[5]

^{1}H Nuclear Magnetic Resonance (^{1}H-NMR)

^{1}H NMR spectra were run on a Bruker DRX300 spectrometer. For a typical experiment, 10 mg of solid was dissolved in a mixture of 0.6 mL of DMSO-d_6 + 0.1 mL D_2SO_4. In case of MIL-100(Ti) solids, further heating at 80 °C with the aid of a magnetic stirrer was needed in order to obtain a clear solution.

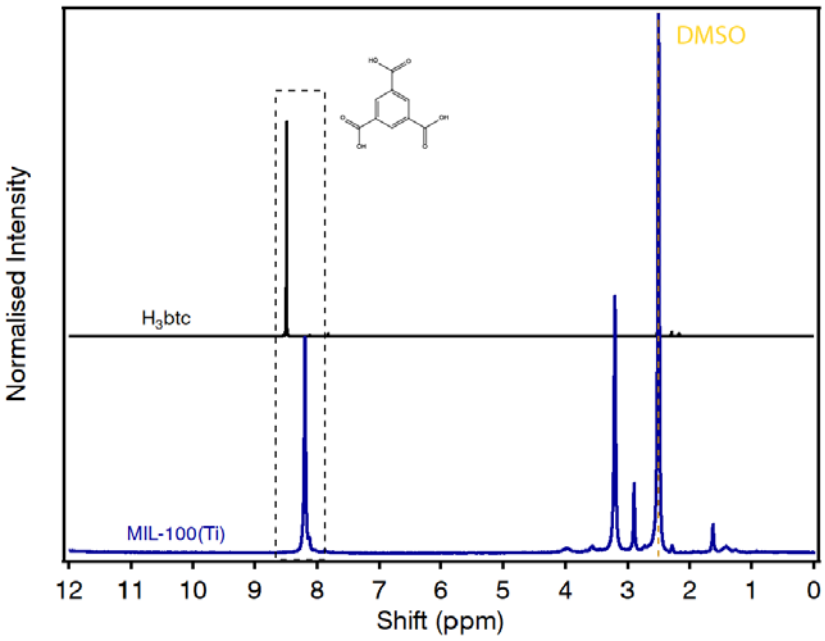

Figure S26. ^{1}H-NMR spectra of digested MIL-100(Ti) (blue) and H_3btc (black).

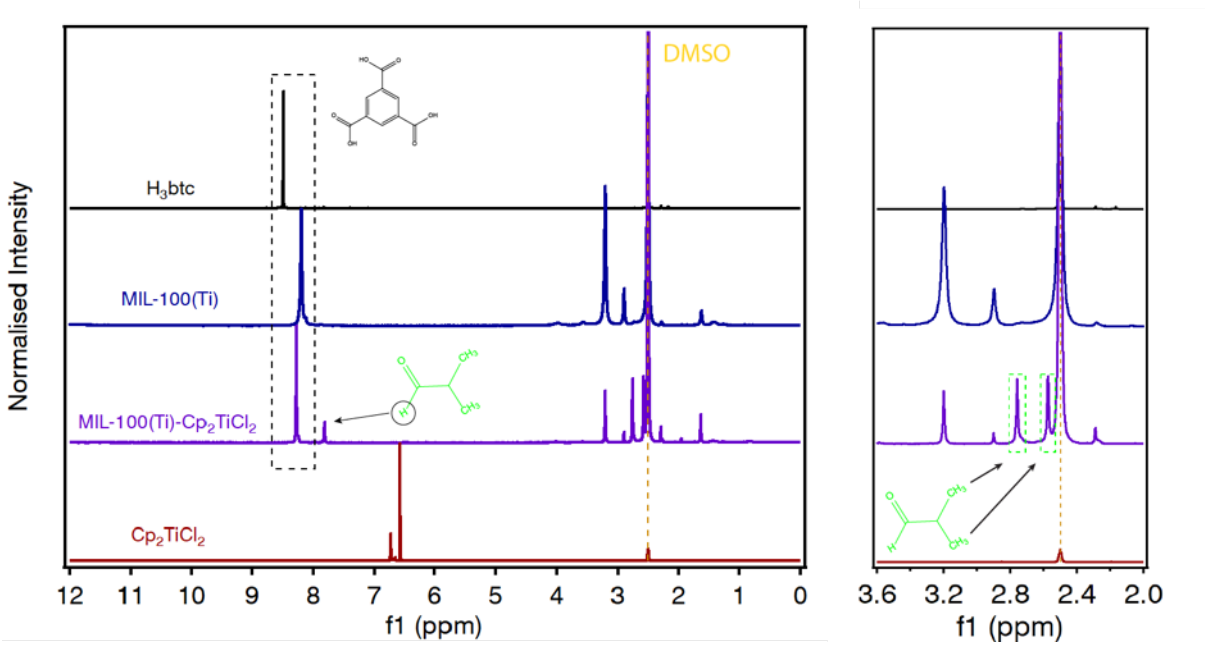

Figure S27. Comparison of the ^{1}H-NMR spectra of digested of MIL-100(Ti)-Cp_2TiCl_2 (purple), Cp_2TiCl_2 (red), MIL-100(Ti) (blue) and H_3btc (black).

^{13}C Cross-Polarization Magic-Angle Spinning Nuclear Magnetic Resonance (^{13}C-CP-MAS-NMR)

CP-MAS-NMR measurements were carried out on a Bruker Avance III 400 WB Spectrometer with 9.4 T field. Samples were loaded in a 4mm zirconia rotor and spun at 8kHz.

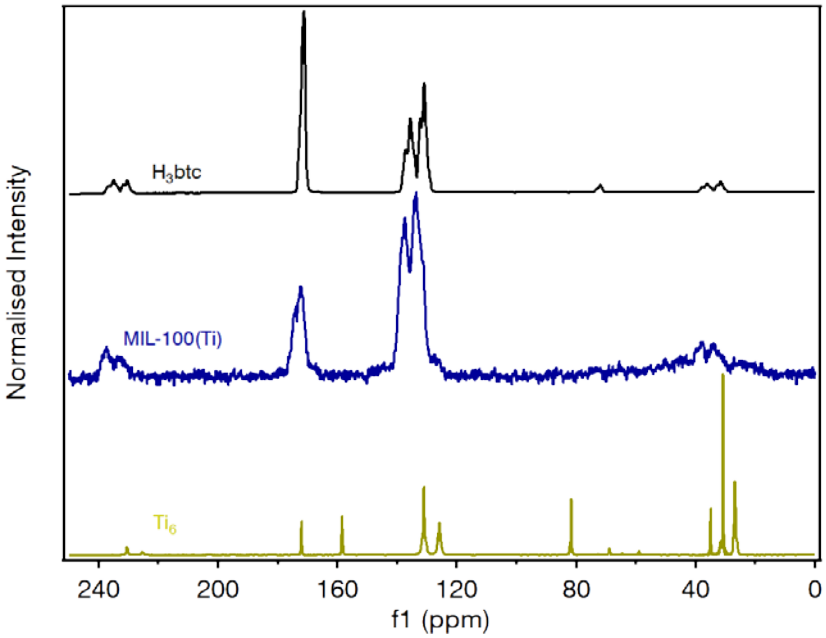

Figure S28. CP-MAS-NMR of the Ti_6 cluster (yellow), MIL-100(Ti) (blue) and H_3btc (black).

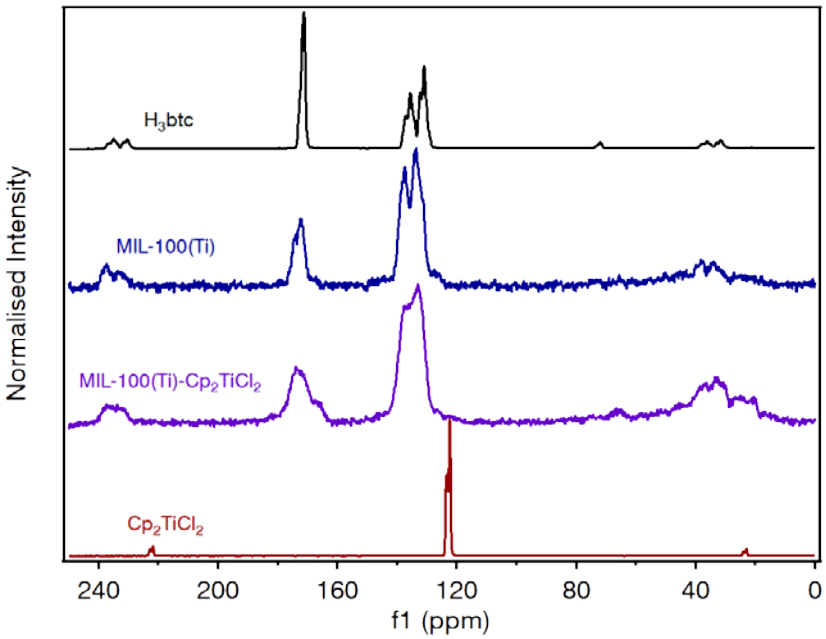

Figure S29. Comparison of the CP-MAS-NMR of MIL-100(Ti)-Cp_2TiCl_2, Cp_2TiCl_2 (red) MIL-100(Ti) (blue) and H_3btc (black) confirming the absence of Cp units in the structure of MIL-100(Ti)-Cp_2TiCl_2.

UV-Vis Spectroscopy – Optical Band-Gap Calculation

UV-Vis diffuse reflectance spectroscopy (DRS) were perfomed on a Jasco V-670 spectrophotometer using an integrated Labsphere in the range 200-800 nm.

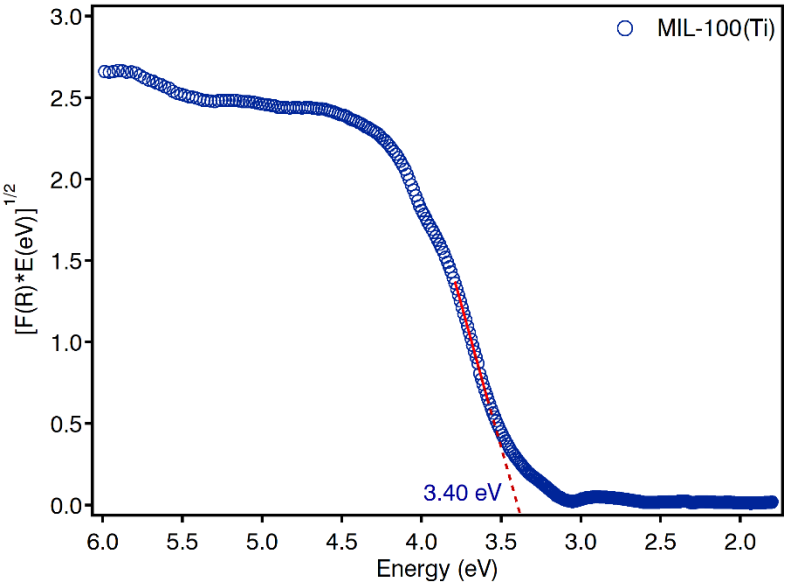

Figure S30. Kubelka-Munk function of and MIL-100(Ti) (blue). The red line corresponds to the regression fitting of the linear part of the plot. The optical band-gap MIL-100(Ti) was calculated to be 3.40 eV.

Electron Paramagnetic Resonance (EPR)

EPR measurements were performed on 20 mg of solid suspended in freshly distilled deoxygenated THF. The samples were degassed prior to experiments by a freeze-pump-thaw procedure and the tube was subsequently flame-sealed. Photoreduction of MIL-100(Ti) was carried out in a Luzchem Photoreactor Model LZC-5 equipped with 8 LZC-UVB lamps. EPR data was recorded in a Bruker ELEXYS E580 spectrometer under X-band irradiation (~ 9.3 GHz) at 77 K.

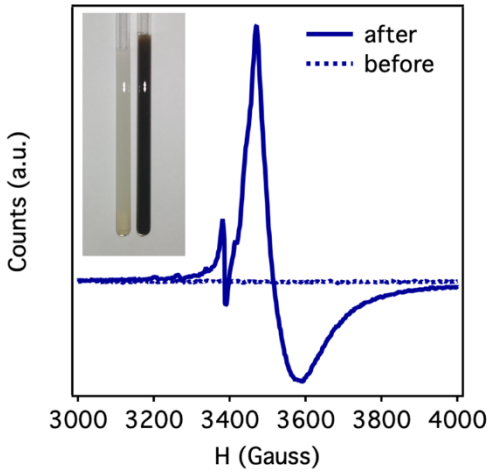

Figure S31. EPR measurement of MIL-100(Ti) before (dashed line) and after irradiation (solid line). The inset shows the change in colour of the solid from white to dark blue after irradiation.

S4. Water Stability of MIL-100 solids

Water stability experiments were carried out by immersing 50 mg of MIL-100(Ti) or MIL-100(Fe) in 5 mL of aqueous solutions of HCl or NaOH at different pH values ranging from 1 to 14. After 24 hours, 1 mL of the solution was separated for ICP-MS measurements and the solution was decanted and the solids washed with water and methanol and allow to dry under dynamic vacuum at room temperature. Chemical stability was confirmed with PXRD and gas sorption measurements of the solids after the treatment.

Powder X-Ray Diffraction of MIL-100(Ti)

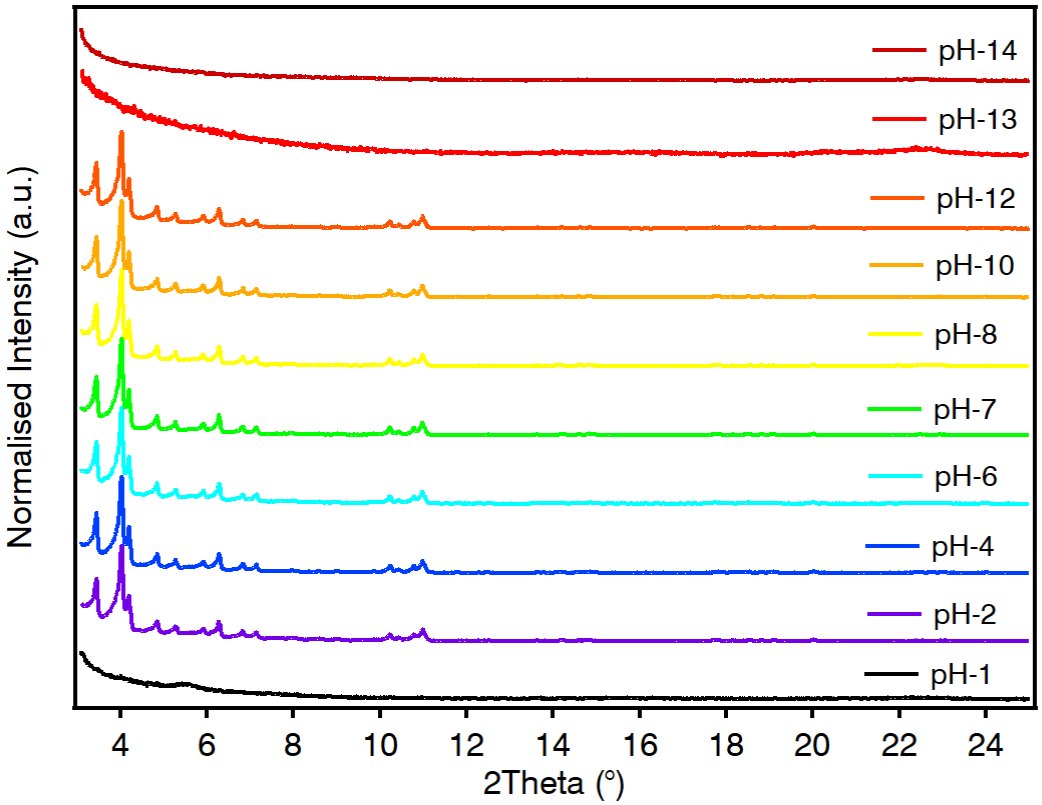

Figure S32. PXRD patterns of MIL-100(Ti) after soaking in aqueous solutions at different pH values for 24 hours.

N_2 adsorption/desorption isotherms at 77 K of MIL-100(Ti)

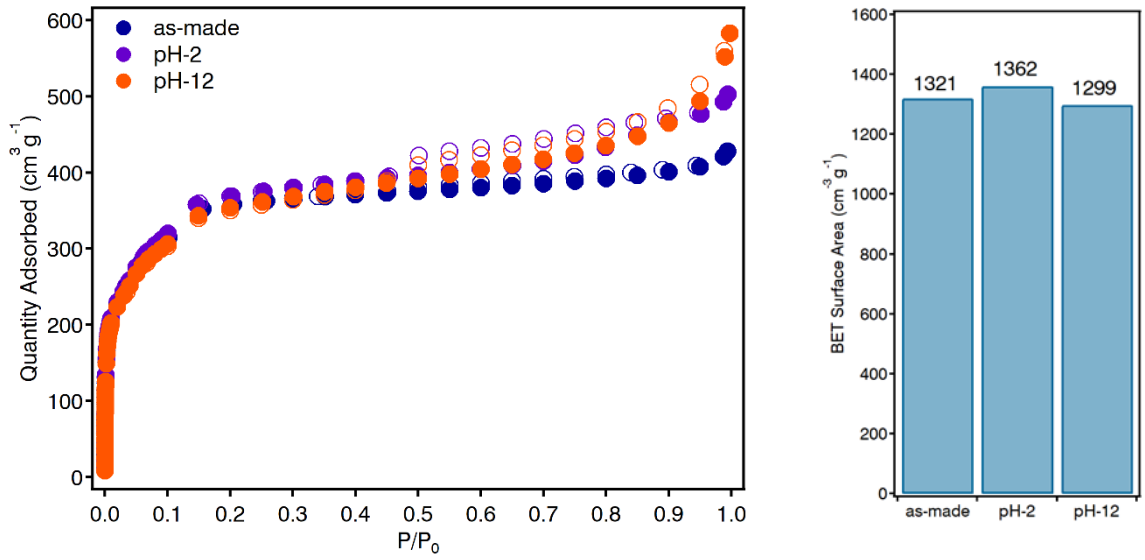

Figure S33. N_2 adsorption/desorption isotherms (left) and calculated BET surface area values (right) of the MIL-100(Ti) solids after treatment at different pH values.

Table S5. Main parameters calculated from the multi-point BET analysis of the MIL-100(Ti) after treatment at different pH values

MIL-100(Ti)	**As-made**	**pH-2**	**pH-12**
BET Area / m^2 g^{-1}	1321.0455 ± 4.2497	1361.9461 ± 5.2380	1299.1180 ± 3.3360
Slope	0.003266 ± 0.000011	0.003164 ± 0.000012	0.003320 ± 0.000009
Intercept	0.000029 ± 0.000001	0.000032 ± 0.000001	0.000031 ± 0.000001
range of P/P_0	0.05 – 0.10	0.05 – 0.10	0.05 – 0.10
R^2	0.99998	0.99998	0.99999
C	113.153	100.850	108.745
V_m / cm^3 g^{-1}	303.509	312.906	298.471
1/(VC+1)	0.08593	0.09056	0.08750
P/P_0 at V_m	0.08621	0.09076	0.08785

Powder X-Ray Diffraction of MIL-100(Fe)

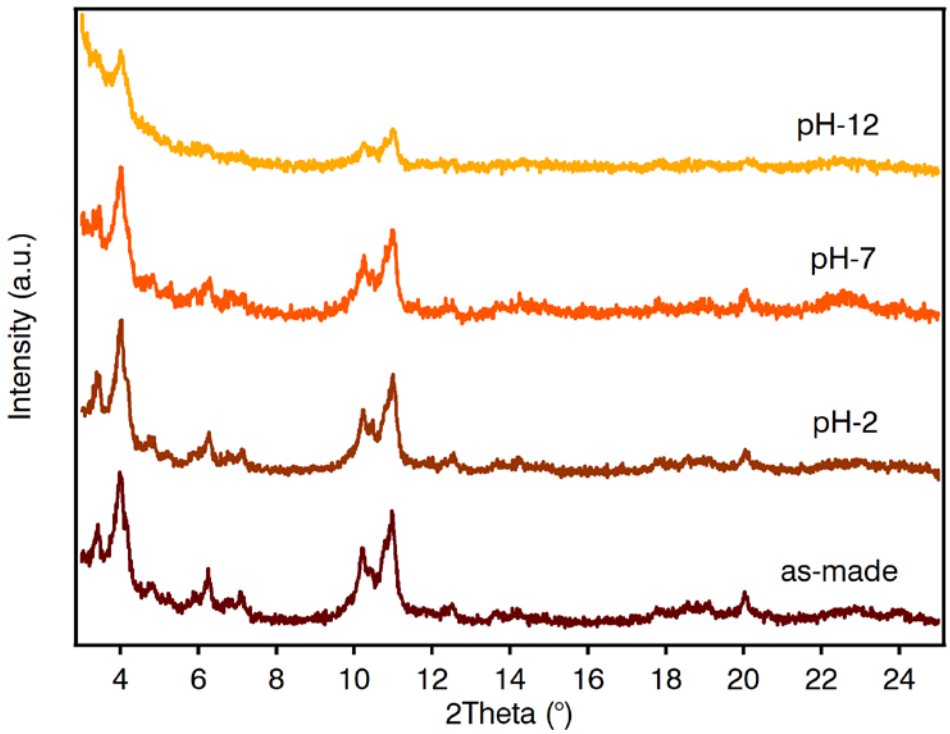

Figure S34. PXRD patterns of MIL-100(Fe) after soaking in aqueous solutions at pH 2, 7 and 12 for 24 hours.

N_2 Adsorption/desorption isotherms at 77K of MIL-100(Fe)

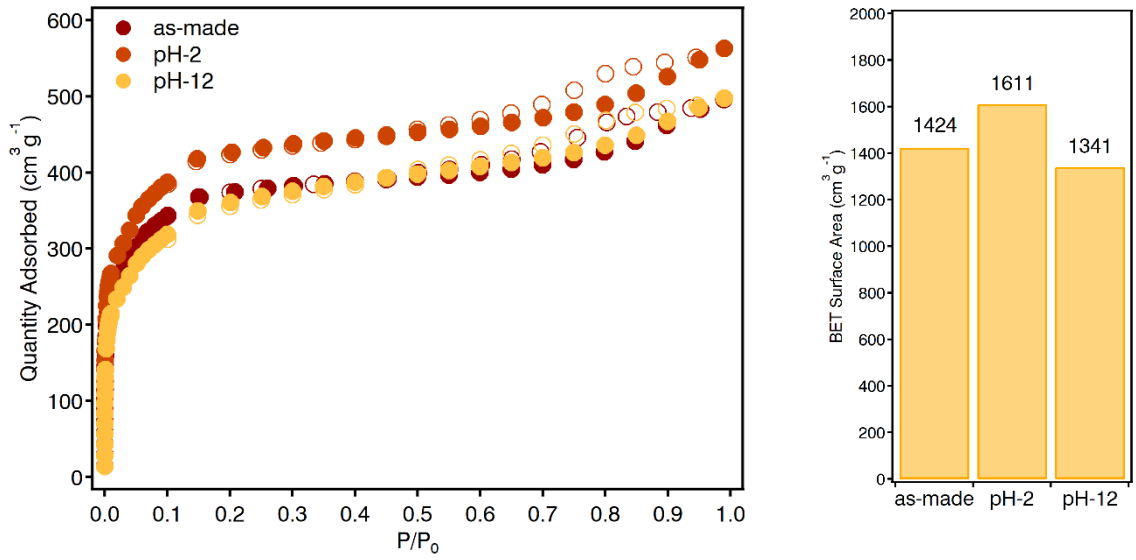

Figure S35. N_2 adsorption/desorption isotherms (left) and calculated BET surface area values (right) of the MIL-100(Fe) solids after water treatment at different pH values.

Table S6. Main parameters calculated from the multi-point BET analysis of the MIL-100(Fe) after water treatment at different pH values

MIL-100(Fe)	**As-made**	**pH-2**	**pH-12**
BET Area / m^2 g^{-1}	1424.0628 ± 2.1866	1611.6591 ± 3.7672	1341.7715 ± 2.0375
Slope	0.0033036 ± 0.000005	0.002682 ± 0.000006	0.003217 ± 0.000005
Intercept	0.000020 ± 0.000000	0.000019 ± 0.000000	0.000027 ± 0.000000
range of P/P_0	0.05 – 0.10	0.05 – 0.10	0.05 – 0.10
R^2	0.99999	0.99999	0.99999
C	150.963	145.975	120.363
V_m / cm^3 g^{-1}	327.177	370.277	308.271
1/(√C+1)	0.07526	0.07644	0.08356
P/P_0 at V_m	0.07497	0.07610	0.08385

Powder X-Ray Diffraction of MIL-125

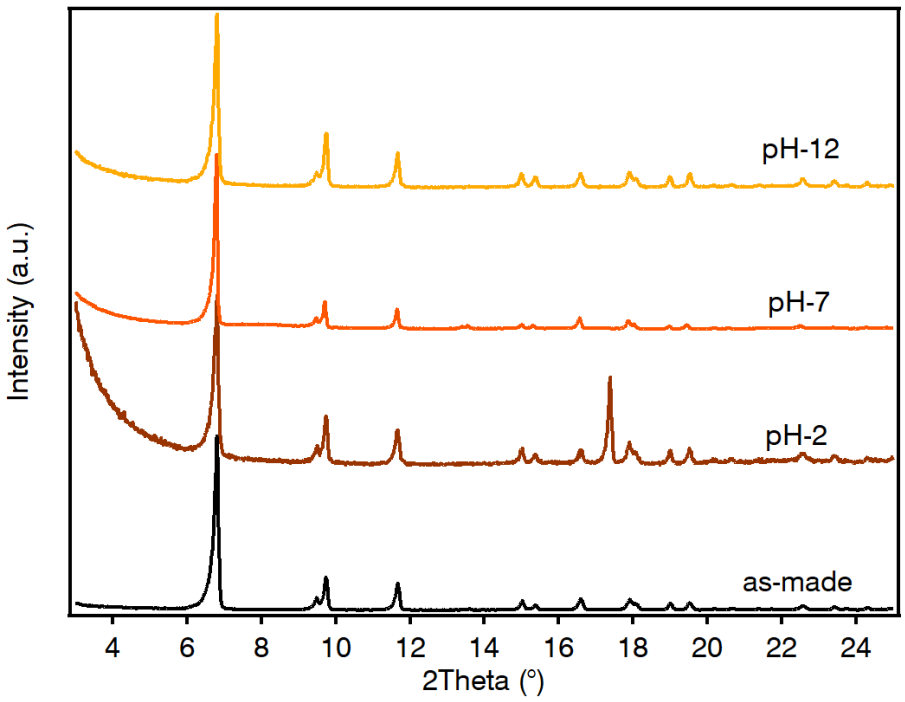

Figure S36. PXRD patterns of MIL-125 after soaking in aqueous solutions at pH 2, 7 and 12 for 24 hours.

N_2 Adsorption/desorption isotherms at 77K of MIL-125

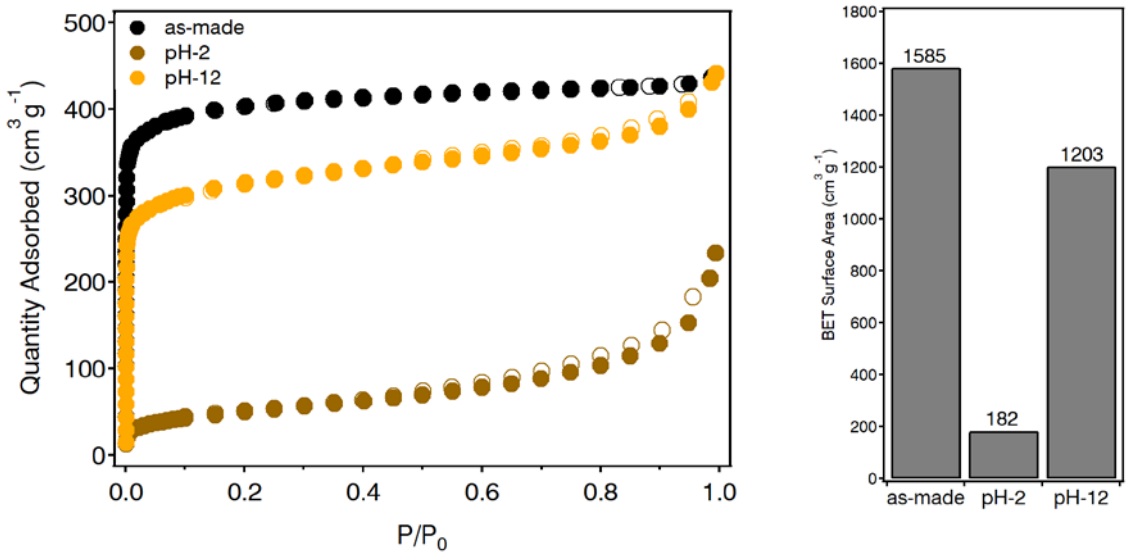

Figure S37. N_2 adsorption/desorption isotherms (left) and calculated BET surface area values (right) of the MIL-125 solids after water treatment at different pH values.

Table S7. Main parameters calculated from the multi-point BET analysis of the MIL-125 after water treatment at different pH values

MIL-125	**As-made**	**pH-2**	**pH-12**
BET Area / m^2 g^{-1}	1585.4173 ± 0.7835	181.5194 ± 0.2708	1202.6511 ± 1.0669
Slope	0.002745 ± 0.000001	0.023762 ± 0.000036	0.003617 ± 0.000003
Intercept	0.000001 ± 0.000000	0.000216 ± 0.000003	0.000002 ± 0.000000
range of P/P_0	0.006 – 0.03	0.05 – 0.15	0.006– 0.04
R^2	0.99999	0.99999	0.99999
C	3279.99	110.902	2125.479
V_m / cm^3 g^{-1}	364.248	41.704	276.308
1/(VC+1)	0.01716	0.08672	0.02123
P/P_0 at V_m	0.01740	0.08697	0.02202

Inductively Coupled Plasma – Mass Spectrometry (ICP-MS) measurements

The determination of Fe and Ti was performed in the aqueous phases of stability tests carried out on MIL-100(Fe) and MIL-100(Ti), respectively, in an Agilent ICP-MS 7900 apparatus.

Table S8. ICP-MS measurements of the concentration of Fe and Ti in the aqueous phase during the stability tests of MIL-100(Fe) and MIL-100(Ti) at different pH values for 24 hours.

	MIL-100(Fe)	**MIL-125**	**MIL-100(Ti)**
pH	**[Fe] (mg·mL^{-1})**	**[Ti] (mg·mL^{-1})**	**[Ti] (mg·mL^{-1})**
2	34.8 ± 0.1	14.1 ± 0.3	0.098 ± 0.001
7	17.1 ± 0.2	0.83 ± 0.03	0.121 ± 0.001

S5. Computational methods

Titanium oxide clusters: geometric structure

Considering the experimental limitation to determine the nature of species occupying the apical position of each Ti octahedron (O^{2-}, OH^- or H_2O), we have used dispersion-corrected density functional theory (DFT-D3)[6,7] as implemented in the Vienna ab initio simulation package (VASP)[8,9] to investigate the best candidate for producing a neutral SBU cluster, using the methodology proposed by De Vos and co-workers.[10] The models of the cluster were derived from a cluster with three apical oxo groups (Figure S34 (top), cMIL-100(Ti)^{3O}), as obtained from refinement of the X-ray diffraction pattern of MIL-100(Ti). The structure was modified with the Materials Studio 2017 R2 package, and the final simulation systems consisted in two hydroxyl ions and one oxo-group c(MIL-100(Ti)^{2OH}) and two oxo-groups and a water molecule c(MIL-100(Ti)^{H_2O}) capped with 6 btc (btc = $OOCC_6H_4COOH$) ligand molecules placed in a box of 25 × 25 × 25 Å^3 size. The atomic positions and total energies were relaxed using the generalized gradient approximation (GGA) with the Perdew–Burke–Ernzerhof (PBE) functional[11] and the hybrid HSE06 functional.[12,13] The kinetic energy cutoff for the plane-wave basis set expansion was chosen as 500 eV, and a Γ-points was used for integrations in the reciprocal space.

Formation energy of the different cluster models

The relative thermodynamic stabilities of these cluster can be calculated in terms of formation energy. It is given by

$$E_f = E_{cluster} - E_{c\mathrm{MIL-100(Ti)}^{3O}} - E_{H_2}$$

where $E_{cluster}$ is the total energy of systems consisted; two hydroxyl ions and one oxo-group c(MIL-100(Ti)^{2OH}) or two oxo-groups and a water molecule c(MIL-100(Ti)^{H_2O}) capped with 6 btc ligand molecules. E_{H_2} is the total energy of a H_2 molecule in *vacuum*. The results are summarized in Table S8.

The use of cyclopentadienyl (Cp) precursors in the synthesis of Ti(IV)-MOFs could result in the presence of Cp units coordinated to the axial positions of the Ti(IV) ions in the trimeric SBU.[10] To further rule out this possibility, we calculated the enthalpy energy of the process of formation of the trimeric Ti(IV) SBU found in MIL-100(Ti) with two Cp units per cluster as follows:

$$E_f = E_{cluster} + 2H_2O - E_{c\mathrm{MIL-100(Ti)}^{3O}} - E_{H_2} - 2E_{HCp}$$

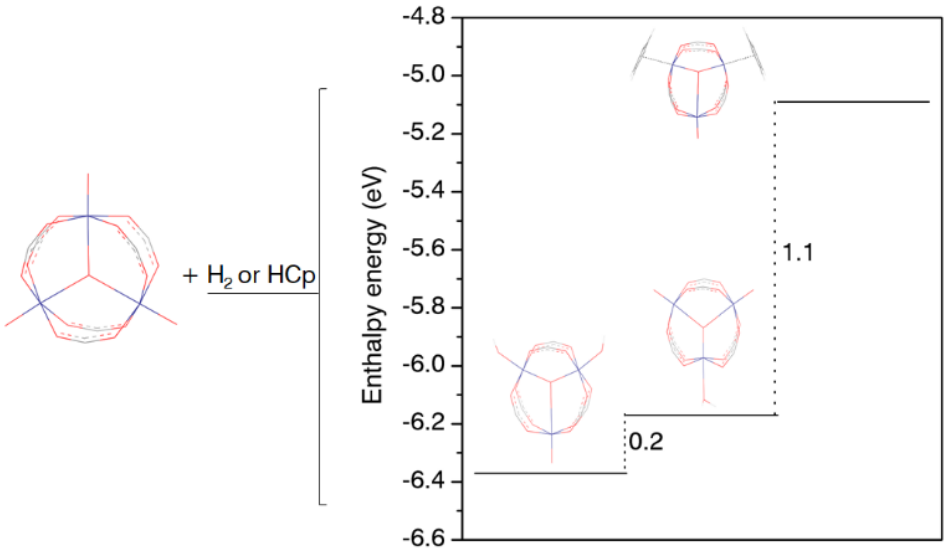

Figure S38. Representation and enthalpy energy of the process of formation for the various possible clusters of MIL-100(Ti).

Table S9. Enthalpy energy of the process of formation for the various possible clusters of MIL-100(Ti) with different functionals.

clusters	E_f (eV/cluster)	
	PBE	HSE06
cMIL-100(Ti)^{3O}	-	-
cMIL-100(Ti)^{2OH}	-6.37	-8.15
cMIL-100(Ti) ^{H_2O}	-6.17	-8.03
cMIL-100(Ti)^{2Cp}	-5.09	-6.82

Simulation of the MIL-100(Ti)-bulk

Based on the obtained formation energies of the clusters, two different structures for MIL-100(Ti) bulk were constructed starting with a primitive unit cell using cell parameters a = b = c = 51.9842 Å, with 68 trimeric Ti(IV) SBU. The neutrality of the cell was maintained by species occupying the apical position of each trimeric Ti(IV) SBU ($2OH^-$ or H_2O) and the charges were dealt with by charge equilibration methods in both systems. These structures were optimized with Materials Studio (MS) Forcite calculations using geometry optimization and extended universal forcefield for metal-organic frameworks (UFF4MOF).[14] The lattice parameters of relaxed structures are shown in Table S6.

Our classical calculations indicate that the energy of crystal structure of MIL-100(Ti)^{2OH} is 12 eV lower than of MIL-100(Ti)^{H_2O} structure, therefore, 0.18 eV/cluster, which is agreement with DFT-D3 clusters calculations.

Table S10. Calculated and refinement lattice parameters of primitive cell of MIL-100(Ti)^{2OH} and MIL-100(Ti)^{H_2O}

Models	a(Å)	b(Å)	c(Å)	α(°)	β(°)	γ(°)
MIL-100(Ti) from Rietveld	51.9842	51.9842	51.9842	60.00	60.00	60.00
MIL-100(Ti)^{2OH}	49.8713	49.8746	49.8540	60.00	59.99	60.01
MIL-100(Ti)^{H_2O}	49.7930	49.7978	49.7875	59.98	60.02	60.04

a)

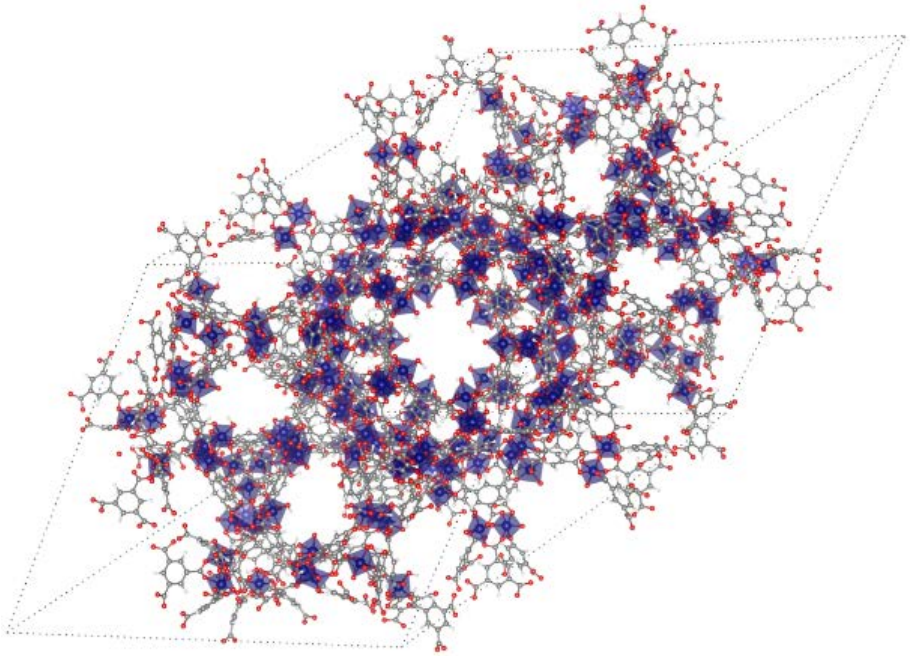

b)

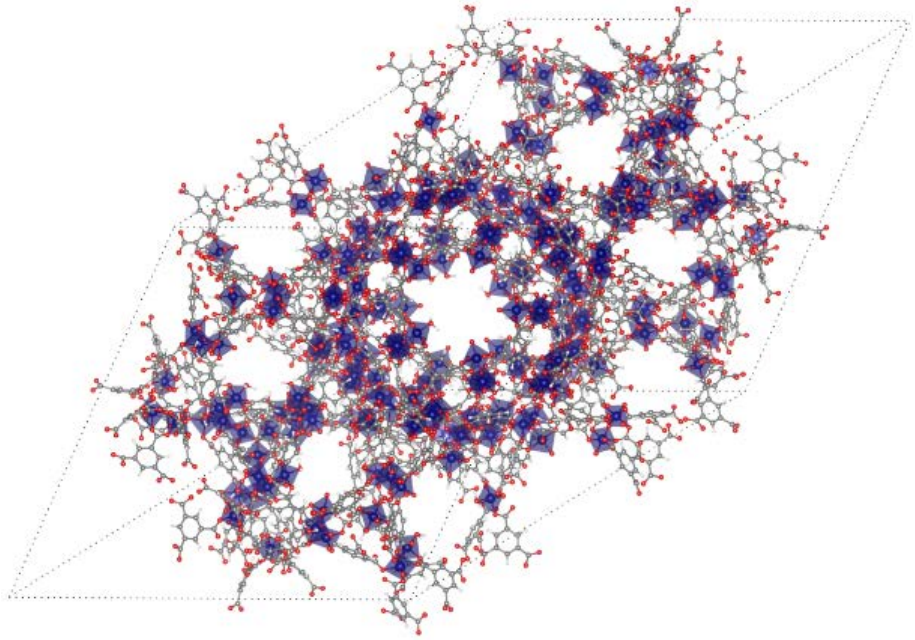

Figure S39. Perspective of the primitive cell of MIL-100(Ti) calculated with: a) two hydroxyl ions and one oxo-group per each trimeric Ti(IV) SBU (MIL-100(Ti)^{2OH}), and b) two oxo-groups and a water molecule per each trimeric Ti(IV) SBU (MIL-100(Ti)^{H_2O}).

S6. Photocatalytic Experiments

Methodology

A quartz photoreactor equipped with a manometer was loaded with sonicated dispersions of the MIL-100(Ti) at 1 mg/mL concentration in H_2O:MeOH (4:1, v/v %) mixture. Prior irradiation the dispersions were purged with Ar for 15 min and pressurized at 1.3 bar. The photoreactor was placed under the spot UV-Vis light of an optical fiber from a 300 W Xe lamp at 100 mW/cm^2. Irradiation was carried out for 24 h.
The H_2 evolution was followed by injecting 250 µL of the reactor gases in an Agilent 490 MicroGC with a TC detector and Ar as carrier gas (MolSieve 5A column). Quantification of the percentage of each gas was based on prior calibration of the system injecting mixtures of H_2 and Ar with known percentage of gases.

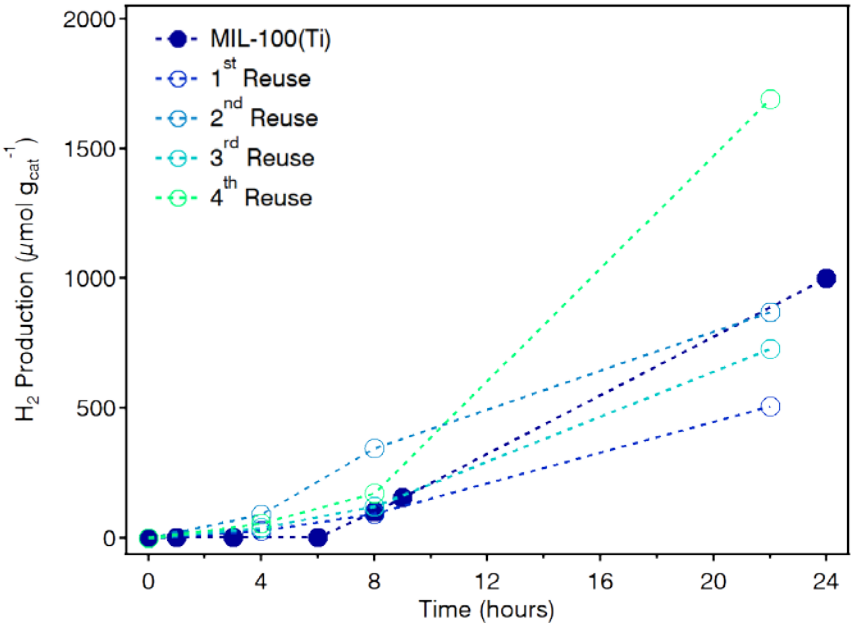

Figure S40. Photocatalytic hydrogen evolution upon consecutive irradiation with a 300 W Xe lamp at 100 mW/cm^2 of 20 mL of a H_2O:MeOH (4:1, v/v %) mixture containing the same MIL-100(Ti) sample.

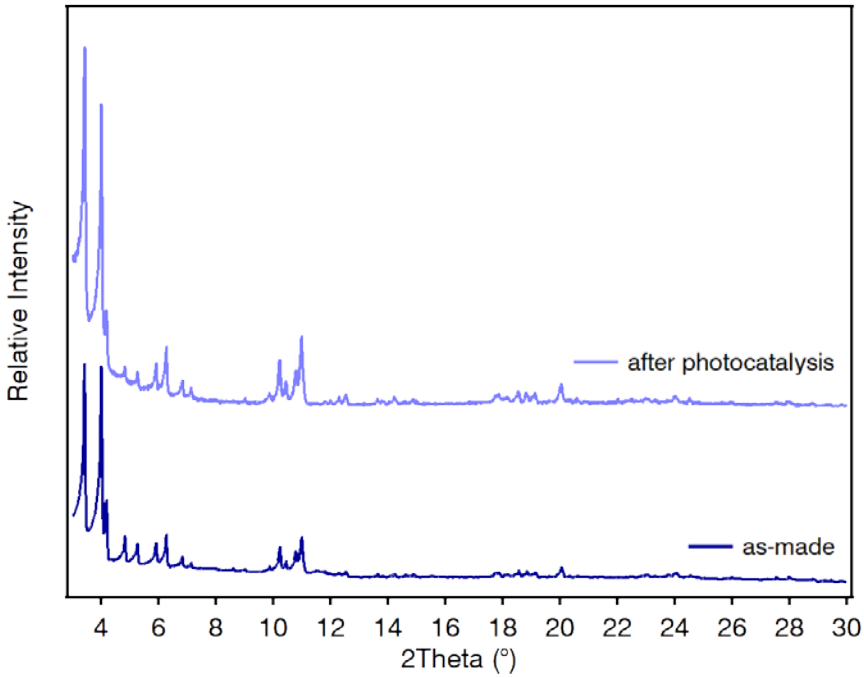

Figure S41. Powder XRD of MIL-100(Ti) before (blue) and after (purple) the photocatalytic experiments.

S7. Transient Absorption Spectroscopy (TAS)

Methodology

Transient absorption spectra were recorded using the forth harmonic of a Q switched Nd:YAG laser (Quantel Brilliant, 266 nm, 15 mJ/pulse, 7 ns fwhm) coupled to a mLFP-122 Luzchem miniaturized detection equipment. This transient absorption spectrometer includes a 300 W ceramic xenon lamp, 125 mm monochromator, Tektronix TDS-2001C digitizer, compact photomultiplier and power supply, cell holder and fiber-optic connectors, computer interfaces, and a software package developed in the LabVIEW environment from National Instruments. The laser flash generates a 5 V trigger pulses with programmable frequency and delay. The rise time of the detector/digitizer is ~3 ns up to 300 MHz (2.5 GHz sampling). The monitoring beam is provided by a ceramic xenon lamp and delivered through fiber-optic cable. The laser pulse is probed by a fiber that synchronizes the photomultiplier detection system with the digitizer operating in the pre-trigger mode.

MIL-100(Ti) was dispersed in ACN **at an approximate concentration of 0.1 mg/mL by sonication for 30 min. Subsequently, the resulting dispersions were purged with Ar for at least 10 min before measurement. Transient signals were monitored at different acquisition times after excitation at 355 nm. Quenching experiments were carried out by monitoring the transient signals of the MOF dispersions upon addition of MeOH (4:1,** v/v %**), and purging with air for 10 min.**

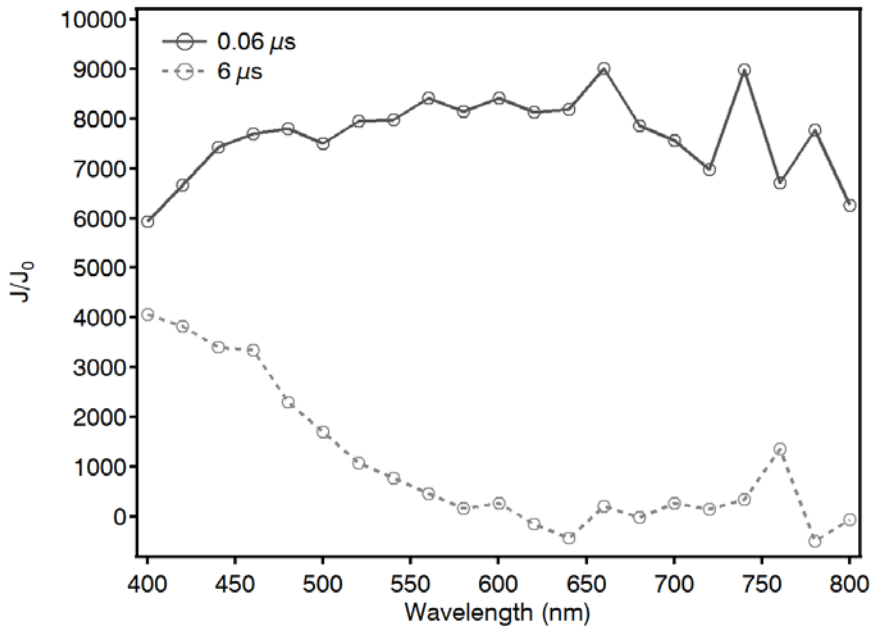

Figure S42. Transient absorption spectra of MIL-100(Ti) suspended in a ACN:MeOH (7:3, v/v %) mixture measured at 0.06 μs (dark grey) and 6 μs after the light pulse.

S8. References

1 K. Hong, W. Bak and H. Chun, *Inorg. Chem.*, 2014, **53**, 7288–7293.
2 R. Canioni, C. Roch-Marchal, F. Sécheresse, P. Horcajada, C. Serre, M. Hardi-Dan, G. Ferey, J.-M. Grenèche, F. Lefebvre, J.-S. Chang, Y. K. Hwang, O. Lebedev, S. Turner and G. Van Tendeloo, *J. Mater. Chem.*, 2011, **21**, 1226–1233.
3 A. J. Howarth, A. W. Peters, N. A. Vermeulen, T. C. Wang, J. T. Hupp and O. K. Farha, *Chem. Mater.*, 2017, **29**, 26–39.
4 M. Wickenheisser, A. Herbst, R. Tannert, B. Milow and C. Janiak, *Micropor. Mesopor. Mat.*, 2015, **215**, 143–153.
5 F. Jeremias, A. Khutia, S. K. Henninger and C. Janiak, *J. Mater. Chem.*, 2012, **22**, 10148–10151.
6 S. Grimme, J. Antony, S. Ehrlich and H. Krieg, *J. Chem. Phys.*, 2010, **132**, 154104.
7 T. Bučko, J. Hafner, S. Lebègue and J. G. Ángyán, *J. Phys. Chem. A*, 2010, **114**, 11814–11824.
8 G. Kresse and J. Furthmüller, *Computational Materials Science*, 1996, **6**, 15–50.
9 G. Kresse and J. Furthmüller, *Phys. Rev. B*, 1996, **54**, 11169–11186.
10 B. Bueken, F. Vermoortele, D. E. P. Vanpoucke, H. Reinsch, C.-C. Tsou, P. Valvekens, T. De Baerdemaeker, R. Ameloot, C. E. A. Kirschhock, V. Van Speybroeck, J. M. Mayer and D. De Vos, *Angew. Chem. Int. Ed.*, 2015, **54**, 13912–13917.
11 J. P. Perdew, K. Burke and M. Ernzerhof, *Phys. Rev. Lett.*, 1996, **77**, 3865–3868.
12 J. Heyd, G. E. Scuseria and M. Ernzerhof, *J. Chem. Phys.*, 2006, **124**, 219906.
13 J. Heyd, G. E. Scuseria and M. Ernzerhof, *J. Chem. Phys.*, 2003, **118**, 8207–8215.
14 M. A. Addicoat, N. Vankova, I. F. Akter and T. Heine, *J. Chem. Theory Comput.*, 2014, **10**, 880–891.